A MODEL OF THE DISTRIBUTION OF MASS IN THE GALACTIC SYSTEM

M. SCHMIDT

A MODEL OF THE DISTRIBUTION OF MASS IN THE GALACTIC SYSTEM

PROEFSCHRIFT

TER VERKRIJGING VAN DE GRAAD VAN DOCTOR IN DE WIS- EN NATUURKUNDE AAN DE RIJKS-UNIVERSITEIT TE LEIDEN, OP GEZAG VAN DE RECTOR MAGNIFICUS DR A. E. VAN ARKEL, HOOGLERAAR IN DE FACULTEIT DER WIS- EN NATUURKUNDE, TEGEN DE BEDENKINGEN VAN DE FACULTEIT DER WIS- EN NATUURKUNDE TE VERDEDIGEN OP WOENSDAG 21 MAART 1956 TE 16 UUR

DOOR

MAARTEN SCHMIDT

GEBOREN TE GRONINGEN IN 1929

1956

PROMOTOR:

PROF. DR J. H. OORT

STELLINGEN

I

De door PARENAGO in een model van het Melkwegstelsel aangegeven potentialen zijn onjuist.

P. P. PARENAGO, *A.J.U.S.S.R.* **29**, 245, 1952.

II

Voor het verkrijgen van enig inzicht in de structuur van het centrale gedeelte van het Melkwegstelsel is het van belang de radiële snelheden van de door BAADE aldaar gevonden RR Lyrae-veranderlijken te kennen.

III

De door LOHMANN uit gepubliceerde lijnprofielen van neutraal waterstof afgeleide spiraalstructuur in het centrale gedeelte van het Melkwegstelsel is ongegrond.

W. LOHMANN, *Zs. f. Ap.* **35**, 90, 1954.

IV

Een nader onderzoek naar de richtingsverdeling van de symmetrie-assen van extragalactische stelsels is gewenst.

F. G. BROWN, *M. N.* **98**, 218, 1938.
F. G. BROWN, *M. N.* **99**, 14, 1938.

V

MCCLAIN's bepaling van de afstand van de radiobron 17S2A (Sagittarius A) kan aan ernstige critiek worden onderworpen.

E. F. MCCLAIN, *Ap. J.* **122**, 376, 1955.

VI

Het al of niet bestaan van een seculaire helderheidsverandering van kometen zal door fotoëlectrische helderheidsbepalingen uitgemaakt kunnen worden.

VII

Bij het verrichten van sommige onderzoekingen wordt vertrouwd op de lineariteit van de karakteristiek van een fotoëlectrische cel met inwendige versterking. Het is wenselijk deze karakteristiek te onderzoeken, indien de stroomafgifte van de cel een bedrag van 10^{-7} A overschrijdt.

G. KORTÜM und H. MAIER, *Zs. f. Naturforschung* **8***a*, 235, 1953.

VIII

De door DOMMANGET gevolgde methode ter bepaling van het begin of het einde van een gedeeltelijke zonsverduistering is onnodig ingewikkeld.

J. DOMMANGET, *Comm. de l'Obs. de Belg.*, No. 78.

IX

MATTHEWS veronderstelt dat duiven, die uit voor hen onbekende streken huiswaarts vliegen, navigeren met behulp van de zon. Dit zou uiterst hoge eisen stellen aan het tijdsgevoel, het bewegingszien en het geheugen van de vogels.

G. V. T. MATTHEWS, *J. Exp. Biol.* **30**, 243, 1953.

X

Bij het vermelden van grote getallen in nieuwsberichten verdient het aanbeveling hieraan vergelijkingscijfers toe te voegen.

XI

Op verkeerspleinen, gelegen op kruispunten van grote verkeerswegen, zullen bij grote drukte opstoppingen ontstaan. Deze kunnen worden vermeden door de pleinen tot voorrangsweg te verheffen.

Aan mijn ouders
Aan mijn vrouw

Op verzoek van de Faculteit der Wis- en Natuurkunde volgt hier een kort overzicht van mijn universitaire studie.

In 1946 begon ik mijn studie te Groningen. Ik volgde de colleges van prof. dr P. J. van Rhijn, destijds gegeven door dr L. Plaut, en de colleges van de professoren dr D. Coster, dr J. C. H. Gerretsen, dr C. S. Meyer en dr J. Ridder. Nadat ik in 1949 het candidaatsexamen (c) had afgelegd, werd ik assistent bij de Sterrewacht te Leiden, waar ik mijn studie voortzette. Hier volgde ik de colleges van de professoren dr H. A. Kramers, dr J. H. Oort en dr H. C. van de Hulst. Ik nam van september 1950 tot october 1951 deel aan de azimuth-expeditie in Kenya onder leiding van dr G. van Herk. Na in 1953 het doctoraal examen te hebben afgelegd, werd ik benoemd tot adjunct wetenschappelijk ambtenaar en een jaar later tot wetenschappelijk ambtenaar bij de Sterrewacht te Leiden.

A MODEL OF THE DISTRIBUTION OF MASS IN THE GALACTIC SYSTEM

The paper deals with the distribution of mass in the Galactic System. Formulae for the potential and forces due to non-homogeneous oblate spheroids are derived (section 2). It is shown that, between the galactic centre and the sun, the central force in the galactic plane decreases almost linearly with the distance from the centre (section 3). A simple analytical expression for the density in a non-homogeneous spheroid is found which gives such a linear decrease of the central force inside the spheroid (section 4). Section 5 summarizes the observational material which forms the basis for the construction of the mass model. A discussion of the values of the constants of differential rotation, A and B, and the distance to the galactic centre, $\varpi_\odot$, is given.

Three models of the distribution of mass are described. Only the third model (section 9) reproduces all we know at present of the system at large. It is shown in section 10 that the second model (section 8) probably does not satisfy conditions of continuity and equilibrium. The third model does not seem to present any difficulties in this respect. A set of nine additional homogeneous spheroids is introduced in section 11 to account for the deviations from a perfectly linear decrease of the central force in the inner part of the system. Together with the third model these form the final model. This final model of the mass distribution is described in section 12. Diagrams and tables of densities, potentials and forces are given for distances up to 17 kpc from the galactic centre. The total mass of the model is $0.70 \times 10^{11}\odot$; the velocity of escape near the sun exceeds the circular velocity by 70 km/sec.

Sections 13 and 14 contain a new discussion of the space and velocity distributions of globular clusters. The system of globular clusters is found to be of ellipsoidal form. The axial ratio of the inner part is about 0.25; it increases to a value near unity in the outer regions. It does not seem possible to draw any reliable conclusions about the differential rotation of the cluster system from the available radial velocities. The average rotational velocity is probably about 80 km/sec.

In the final section the force exerted by a spiral arm, such as that found in the vicinity of the sun, has been estimated.

1. *Introduction.*

The present paper contains a study of the distribution of mass in the Galactic System. A recent determination [1]) of the rotational velocities up to 8.2 kpc from the centre, from observed maximum radial velocities of neutral hydrogen at 21-cm wave length, offers promising possibilities for such an investigation.

Several authors have constructed models of the mass distribution. OORT has published some models, of which the most recent one was given in his Russell Lecture [2]). It consists of seven homogeneous spheroids. A disadvantage of the homogeneous spheroids is the discontinuity of the derivative of the force at the boundary. WYSE and MAYALL [3]), in a study of the rotational velocities in extragalactic nebulae, used a plane circular disc in which the density changes gradually outwards. PEREK [4]) combined the advantages of both representations and introduced the non-homogeneous spheroid. The density laws he assumed are arbitrary, however. PARENAGO [5]) derived a model which is based on the assumption that the velocity distributions are ellipsoidal everywhere in the system.

In the present investigation non-homogeneous spheroids will be used. Formulae for the general case are given in section 2. In the following section it is shown that between the centre and the sun the force in the galactic plane decreases approximately linearly with distance. The same property applies inside a non-homogeneous spheroid if a specific density law in the spheroid is assumed. With this density law, formulae for potential and forces are developed which form the basis of all further calculations.

Throughout this paper a unit of length of 1 kpc and a unit of velocity of 1 km/sec will be used. The resulting units of potential, force, mass density and mass are given below; γ is the constant of gravitation. If a number is given without specifying a unit, it is expressed in one of the units listed. It is to be noted that the force used in this paper is a force per unit mass, i.e. an acceleration.

Unit of length	1 kpc
Unit of velocity	1 km/sec
Unit of potential	1 km^2/sec^2
Unit of force	1 $km^2/sec^2.kpc$
	$= 3.24 \times 10^{-12}$ cm/sec^2
Unit of mass density	$\frac{1}{\gamma}$ $km^2/sec^2.kpc^2$
	$= 1.578 \times 10^{-26}$ gr/cm^3
	$= 2.32 \times 10^{-4}\odot/ps^3$.
Unit of mass	$\frac{1}{\gamma}$ kpc. km^2/sec^2
	$= 4.63 \times 10^{38}$ gr
	$= 2.32 \times 10^{5}\odot$.

---

[1]) K. K. KWEE, C. A. MULLER and G. WESTERHOUT, *B.A.N.* **12**, 211, 1954; No. 458.

[2]) J. H. OORT, *Ap. J.* **116**, 233, 1952.

[3]) A. B. WYSE and N. U. MAYALL, *Ap. J.* **95**, 5, 1942.

[4]) L. PEREK, *Contr. Astr. Inst. Masaryk Univ.* I, No. 6, 1948.

[5]) P. P. PARENAGO, *A. J. U.S.S.R.* **27**, 329, 1950 and **29**, 245, 1952.

A list of the most important symbols is given below. Suffices 1, 2, ... refer to mass spheroids, so that ρ_2 is the density in the second spheroid. A suffix o always refers to the neighbourhood of the sun, e.g. ρ_o is the density near the sun. The density near the sun in a spheroid is indicated by two suffices, e.g. ρ_{20}.

R	distance to the galactic centre,
ϖ	distance to the galactic axis of rotation,
z	distance to the galactic plane,
K_ϖ	component of the force, projected on the galactic plane,
K_z	component of the force, parallel to the galactic axis of rotation,
Φ	potential,
$\rho_n (n = 1, 2, \ldots)$	mass density in the n^{th} spheroid,
ρ_o	mass density near the sun,
ρ_{no}	mass density near the sun in the n^{th} spheroid,
a	equatorial semi-axis of a spheroid,
e	eccentricity of a spheroid,
a_r	equatorial semi-axis of a non-homogeneous spheroid,
p, q	constants in the expression (4,2) for the density ρ,
P, Q	constants in the expression (3,2) for the force K_ϖ in the galactic plane.

2. *General theory of the potential of an oblate non-homogeneous spheroid.*

At first we shall confine ourselves to the potential and forces of a homogeneous oblate spheroid. The theory has been developed mainly by the work of GAUSS and DIRICHLET. A short derivation has been given by HEYMANN [1]). We shall use co-ordinates ϖ and z measured from the centre in a plane through the axis of rotation of the spheroid, ϖ being measured in the equatorial plane and z parallel to the axis. Then, if a and c are the equatorial and polar semi-axes of the spheroid, respectively (with $c < a$) and ρ the uniform density, the potential is

$$\Phi = \pi\rho a^2 c \int_\lambda^\infty \left(1 - \frac{\varpi^2}{a^2+u} - \frac{z^2}{c^2+u}\right) \frac{du}{(a^2+u)\sqrt{c^2+u}}. \tag{2,1}$$

For a point inside the spheroid

$$\lambda = 0, \tag{2,2}$$

while for a point outside the spheroid, λ is the positive root of

$$\frac{\varpi^2}{a^2+\lambda} + \frac{z^2}{c^2+\lambda} = 1. \tag{2,3}$$

We have omitted a minus sign in (2,1) so that the potential is always positive, contrary to the conventional definition of Φ. The force component K_ϖ parallel to the ϖ-axis is

$$K_\varpi = -\frac{\partial\Phi}{\partial\varpi} = 2\pi\rho a^2 c\varpi \int_\lambda^\infty \frac{du}{(a^2+u)^2\sqrt{c^2+u}}$$

$$- \pi\rho a^2 c \frac{\partial\lambda}{\partial\varpi}\left(1 - \frac{\varpi^2}{a^2+\lambda} - \frac{z^2}{c^2+\lambda}\right) \frac{1}{(a^2+\lambda)\sqrt{c^2+\lambda}}.$$

The last term vanishes for all points, whether inside or outside, because of (2,2) and (2,3), so

$$K_\varpi = 2\pi\rho a^2 c\varpi \int_\lambda^\infty \frac{du}{(a^2+u)^2\sqrt{c^2+u}}, \tag{2,4}$$

and similarly

$$K_z = 2\pi\rho a^2 c z \int_\lambda^\infty \frac{du}{(a^2+u)(c^2+u)\sqrt{c^2+u}}, \tag{2,5}$$

so that

$$\Phi = \pi\rho a^2 c \int_\lambda^\infty \frac{du}{(a^2+u)\sqrt{c^2+u}} - \tfrac{1}{2}(\varpi K_\varpi + z K_z). \tag{2,6}$$

We now introduce a new variable

$$\alpha = \arcsin \frac{ae}{\sqrt{a^2+u}}, \tag{2,7}$$

where e is the eccentricity

$$e = \sqrt{1 - \frac{c^2}{a^2}}. \tag{2,8}$$

Then,
$$a^2 + u = a^2 e^2 \operatorname{cosec}^2\alpha,$$
$$c^2 + u = a^2 e^2 \operatorname{cotg}^2\alpha.$$

Let
$$a^2 + \lambda = a^2 e^2 \operatorname{cosec}^2\beta,$$
$$c^2 + \lambda = a^2 e^2 \operatorname{cotg}^2\beta,$$

then (2,2) is equivalent with

$$\sin\beta = e, \tag{2,9}$$

and (2,3) with

$$\varpi^2 \sin^2\beta + z^2 \operatorname{tg}^2\beta = a^2 e^2. \tag{2,10}$$

With these substitutions the integrals of (2,4) to (2,6) are easily evaluated, and we obtain

$$K_\varpi = 2\pi e^{-3}\sqrt{1-e^2}\,\rho\varpi(\beta - \sin\beta\cos\beta), \tag{2,11}$$

$$K_z = 4\pi e^{-3}\sqrt{1-e^2}\,\rho z(\operatorname{tg}\beta - \beta), \tag{2,12}$$

$$\Phi = 2\pi e^{-1}\sqrt{1-e^2}\,\rho a^2\beta - \tfrac{1}{2}(\varpi K_\varpi + z K_z). \tag{2,13}$$

Inside the spheroid, β is given by (2,9), and outside by (2,10). Formulae (2,9) to (2,13) give a complete description of the potential and force fields of a *homogeneous* spheroid.

We shall now consider a *non-homogeneous* spheroid. This can be built up by an infinite number of homogeneous spheroids with varying a and of density $d\rho$.

[1]) O. HEYMANN, *A.N.* **256**, 181, 1935.

We confine ourselves to the case where the eccentricity e of all the elementary spheroids is equal. Then

$$dK_\varpi = 2\pi e^{-3}\sqrt{1-e^2}\,\varpi\,(\beta - \sin\beta\cos\beta)\,d\rho, \quad \text{etc.}$$

The situation is somewhat complicated because we now have three variables, which are ρ, a and β. It should be noted that ϖ and z are not variable, because they are co-ordinates of some fixed point in which we want to compute potential and forces. Inside a homogeneous elementary spheroid, β is constant because of (2,9), while outside, β decreases monotonously with decreasing a, by (2,10). Inside the non-homogeneous spheroid the density ρ is supposed to decrease monotonously with increasing a, while $\rho = 0$ outside. It is possible to make each of the three variables ρ, a and β an integration variable in turn, provided due account is taken of the above considerations.

We shall first consider a fixed point (ϖ,z) *inside* the non-homogeneous spheroid. Let the density at that point be $\rho(\varpi,z)$. Then $\rho(\varpi,z)$ is the sum of the densities of all the elementary homogeneous spheroids containing the point considered. For these homogeneous spheroids β is given by (2,9), while for all other homogeneous spheroids β is given by (2,10).

Then

$$K_\varpi = 2\pi e^{-3}\sqrt{1-e^2}\,\varpi\left\{(\arcsin e - e\sqrt{1-e^2})\,\rho(\varpi,z) + \int_{\rho(\varpi,z)}^{\rho_c}(\beta - \sin\beta\cos\beta)\,d\rho\right\}, \tag{2,14}$$

where ρ_c is the density in the centre of the non-homogeneous spheroid, while β is determined by (2,10). Interchanging the variables ρ and β in the integral, we obtain

$$\int_{\rho(\varpi,z)}^{\rho_c}(\beta - \sin\beta\cos\beta)\,d\rho = (\beta - \sin\beta\cos\beta)\,\rho\Big|_{\rho=\rho(\varpi,z)}^{\rho=\rho_c} - \int_{\arcsin e}^{0}\rho\frac{d}{d\beta}(\beta - \sin\beta\cos\beta)\,d\beta$$

$$= -(\arcsin e - e\sqrt{1-e^2})\,\rho(\varpi,z) + 2\int_0^{\arcsin e}\rho\sin^2\beta\,d\beta.$$

Thus

$$K_\varpi = 4\pi e^{-3}\sqrt{1-e^2}\,\varpi\int_0^{\arcsin e}\rho\sin^2\beta\,d\beta, \tag{2,15}$$

and

$$K_z = 4\pi e^{-3}\sqrt{1-e^2}\,z\int_0^{\arcsin e}\rho\,\mathrm{tg}^2\beta\,d\beta. \tag{2,16}$$

The potential becomes

$$\Phi = 2\pi e^{-1}\sqrt{1-e^2}\left\{\arcsin e\int_0^{\rho(\varpi,z)}a^2\,d\rho + \int_{\rho(\varpi,z)}^{\rho_c}a^2\beta\,d\rho\right\} - \tfrac{1}{2}(\varpi K_\varpi + zK_z), \tag{2,17}$$

β being again determined by (2,10).

Now

$$\int_0^{\rho(\varpi,z)}a^2\,d\rho = \rho a^2\Big|_{\rho=0}^{\rho=\rho(\varpi,z)} - \int_{a_r}^{a(\varpi,z)}2\rho a\,da$$

$$= \rho(\varpi,z)\,a^2(\varpi,z) - \int_{a_r}^{a(\varpi,z)}2\rho a\,da,$$

where $a(\varpi,z)$ is the value of a corresponding to $\rho = \rho(\varpi,z)$. Formally $a(\varpi,z)$ is the semi-axis of the elementary homogeneous spheroid passing through the point (ϖ,z) considered, so that $\sin\beta = e$ and by (2,10)

$$a^2(\varpi,z) = \varpi^2 + \frac{z^2}{1-e^2}. \tag{2,18}$$

a_r is the value of a corresponding to $\rho = 0$, i.e. to the boundary of the non-homogeneous spheroid.

Further

$$\frac{d(a^2\beta)}{da} = 2a\beta + a^2\frac{d\beta}{da},$$

so

$$\int_{\rho(\varpi,z)}^{\rho_c}a^2\beta\,d\rho = \rho a^2\beta\Big|_{\rho=\rho(\varpi,z)}^{\rho=\rho_c} - \int_{a(\varpi,z)}^{0}2\rho a\beta\,da - \int_{\arcsin e}^{0}\rho a^2\,d\beta$$

$$= -\rho(\varpi,z)\,a^2(\varpi,z)\arcsin e + 2\int_0^{a(\varpi,z)}\rho a\beta\,da + \int_0^{\arcsin e}\rho a^2\,d\beta.$$

From (2,15) and (2,16) we find

$$\tfrac{1}{2}(\varpi K_\varpi + zK_z) = 2\pi e^{-1}\sqrt{1-e^2}\int_0^{\arcsin e}\rho a^2\,d\beta,$$

so that, finally,

$$\Phi = 4\pi e^{-1}\sqrt{1-e^2}\left[\int_0^{a(\varpi,z)}\rho a\beta\,da + \arcsin e\int_{a(\varpi,z)}^{a_r}\rho a\,da\right]. \tag{2,19}$$

We shall now consider a point (ϖ,z) *outside* the non-homogeneous spheroid. Then the density $\rho(\varpi,z) = 0$, so that the first term of (2,14) vanishes. The integral has then to be integrated over the range $\rho = 0$ to $\rho = \rho_c$, which is equivalent to the interval from $a = a_r$ to $a = 0$, or $\beta = \gamma$ to $\beta = 0$, where γ is given by substituting $a = a_r$ in (2,10):

$$\varpi^2 \sin^2\gamma + z^2 \operatorname{tg}^2\gamma = a_r^2 e^2. \qquad (2,20)$$

We thus obtain

$$K_\varpi = 4\pi e^{-3}\sqrt{1-e^2}\,\varpi \int_0^\gamma \rho \sin^2\beta \, d\beta, \qquad (2,21)$$

and

$$K_z = 4\pi e^{-3}\sqrt{1-e^2}\, z \int_0^\gamma \rho \operatorname{tg}^2\beta \, d\beta, \qquad (2,22)$$

where β is again given by (2,10).
In a similar way the potential becomes

$$\Phi = 4\pi e^{-1}\sqrt{1-e^2} \int_0^{a_r} \rho a \beta \, da. \qquad (2,23)$$

Thus we have obtained the potential and forces of a non-homogeneous spheroid for internal points in (2,10), (2,15), (2,16) and (2,19) and for external points in (2,10), (2,20) to (2,23). Internal points have $a(\varpi,z) < a_r$ and external points $a(\varpi,z) > a_r$. It should be noted that in the derivation of the formulae the value of ρ_c has been considered to be finite. However, the results remain valid as long as the density in the centre does not become infinite with a degree higher than three.

3. *The observed force in the galactic plane.*

We shall now study the run of the central force as observed in the galactic plane and investigate whether it may be expressed analytically with some accuracy. Important information about the force in the galactic plane in the inner part of the system may be derived from the rotational velocities of neutral hydrogen obtained by KWEE, MULLER and WESTERHOUT [1]. These rotational velocities were computed from the maximum radial velocities observed at 21-cm wave length at different galactic longitudes. Recent Australian observations [2] at longitudes south of the galactic centre show roughly the same maximum radial velocities as found at the corresponding northern longitudes. We shall assume that the rotational velocities represent circular velocities Θ_c. The central force K_ϖ is then

$$K_\varpi = \frac{\Theta_c^2}{\varpi} = \varpi\,\omega^2. \qquad (3,1)$$

[1] *Loc. cit.*
[2] Private communication by F. J. KERR.

The values of K_ϖ computed for 8 points about 1 kpc apart are given in Table 1, together with the angular

TABLE 1
Comparison between the observed force and the analytical approximation.

ϖ kpc	ω km/sec. kpc	K_ϖ km²/sec².kpc	K_ϖ (comp.) km²/sec².kpc	deviation km²/sec².kpc
0.84	163	22300	15700	+ 6600
1.90	91.6	15900	14300	+ 1600
2.93	66.9	13110	12890	+ 220
3.90	53.6	11200	11570	− 370
5.09	43.0	9410	9950	− 540
6.13	36.7	8260	8540	− 280
7.16	31.4	7060	7130	− 70
8.20	26.4	5720	5720	0

velocities, $\omega = \dfrac{\Theta_c}{\varpi}$, from which they were derived. It is found that K_ϖ decreases about linearly with increasing ϖ, so

$$K_\varpi = P\varpi + Q, \qquad (3,2)$$

where $P < 0$. The fourth column of Table 1 gives the computed values of K_ϖ for $P = -1362$ and $Q = 16885$. These particular values of P and Q will be explained in section 5. The representation of the observed values is quite good: between $\varpi = 2.5$ and 8.2 kpc the deviations never exceed 6%. It seems worth while, therefore, to extend the formulation of section 2 to the special case of a force law (3,2).

4. *Development of formulae for a specific force law.*

Let us suppose that inside a non-homogeneous spheroid the force in the equatorial plane decreases linearly with distance, as given in (3,2). We may apply equation (2,15), so that

$$P\varpi + Q = 4\pi e^{-3}\sqrt{1-e^2}\,\varpi \int_0^{\arcsin e} \rho \sin^2\beta \, d\beta, \qquad (4,1)$$

where, according to (2,10) with $z = 0$, $\sin\beta = \dfrac{ae}{\varpi}$.
It may easily be seen that the density law

$$\rho = p + \frac{q}{a} \qquad (4,2)$$

satisfies the integral equation (4,1). Substitution yields

$$P\varpi + Q = 4\pi e^{-3}\sqrt{1-e^2}\left\{\tfrac{1}{2}p\varpi\left(\arcsin e - e\sqrt{1-e^2}\right) + qe\left(1-\sqrt{1-e^2}\right)\right\}.$$

This expression should apply to all internal points $(\varpi,0)$, so that

$$\left.\begin{aligned} P &= 2\pi e^{-3}\sqrt{1-e^2}\,(\arcsin e - e\sqrt{1-e^2})\,p, \\ Q &= 4\pi e^{-2}\sqrt{1-e^2}\,(1-\sqrt{1-e^2})\,q. \end{aligned}\right\} \quad (4,3)$$

Thus, for a force law of the type (3,2), the parameters p and q of the density law only depend on the eccentricity e.

Formula (4,2) gives the space density on the surface of a spheroid with semi-axis a and eccentricity e. The density at a point (ϖ,z) is obtained by substituting

$$a(\varpi,z) = \sqrt{\varpi^2 + \frac{z^2}{1-e^2}} \text{ in (4,2).}$$

The boundary of the non-homogeneous spheroid in most cases has been defined as the surface with $\rho = 0$. This surface is a spheroid with semi-axis a_r, which is given by

$$a_r = -\frac{q}{p}. \quad (4,4)$$

In a few cases the boundary of the non-homogeneous spheroid was taken to be a surface with $\rho = \text{const.} > 0$, in which case (4,4) does not apply. It will appear in subsequent sections that a_r is larger than the distance of the sun from the galactic centre (8.2 kpc). The density law (4,2) thus yields a force law (3,2) in the galactic plane up to $\varpi = 8.2$ kpc. We shall now substitute the density law (4,2) in the formulae developed in section 2.

We consider first a point $(\varpi,0)$ *in* the galactic plane. In the plane $z = 0$, so from (2,10)

$$\sin\beta = \frac{ae}{\varpi}.$$

From (2,21)
$$K_\varpi = 4\pi e^{-3}\sqrt{1-e^2}\,\varpi \int_0^\gamma \left(p + \frac{qe}{\varpi\sin\beta}\right)\sin^2\beta\,d\beta,$$

or
$$K_\varpi = 4\pi e^{-3}\sqrt{1-e^2}\,\varpi\left\{\tfrac{1}{2}p(\gamma - \sin\gamma\cos\gamma) + \frac{qe}{\varpi}(1-\cos\gamma)\right\}, \quad (4,5)$$

and similarly
$$K_z = 4\pi e^{-3}\sqrt{1-e^2}\,z\left\{p(\operatorname{tg}\gamma - \gamma) + \frac{qe}{\varpi}(\sec\gamma - 1)\right\}, \quad (4,6)$$

where
$$\sin\gamma = \frac{a_r e}{\varpi} \quad \text{if} \quad \varpi > a_r, \qquad \sin\gamma = e \quad \text{if} \quad \varpi \leq a_r. \quad (4,7)$$

In the galactic plane $K_z = 0$, by reasons of symmetry, so that (4,6) becomes an identity. But it may be used to compute $\frac{\partial K_z}{\partial z}$, $\frac{\partial K_z}{\partial \varpi}$ and K_z for points near the galactic plane, i.e. $z < 0.1$ kpc. According to equation (2,19) the potential for an internal point is

$$\Phi = 4\pi e^{-1}\sqrt{1-e^2}\left[\int_0^\varpi \left(p + \frac{q}{a}\right)\arcsin\frac{ae}{\varpi}\,a\,da + \arcsin e\int_\varpi^{a_r}\left(p+\frac{q}{a}\right)a\,da\right] \quad (4,8)$$

$$= 4\pi e^{-1}\sqrt{1-e^2}\left\{\tfrac{1}{2}p\frac{\varpi^2}{e^2}\left(\frac{a_r^2e^2}{\varpi^2}\arcsin e - \tfrac{1}{2}\arcsin e + \tfrac{1}{2}e\sqrt{1-e^2}\right) + q\frac{\varpi}{e}\left(\frac{a_r e}{\varpi}\arcsin e + \sqrt{1-e^2} - 1\right)\right\},$$

while for an external point, by (2,23)

$$\Phi = 4\pi e^{-1}\sqrt{1-e^2}\int_0^{a_r}\left(p+\frac{q}{a}\right)\arcsin\frac{ae}{\varpi}\,a\,da \quad (4,9)$$

$$= 4\pi e^{-1}\sqrt{1-e^2}\left\{\tfrac{1}{2}p\frac{\varpi^2}{e^2}\left(\frac{a_r^2e^2}{\varpi^2}\gamma - \tfrac{1}{2}\gamma + \tfrac{1}{2}\sin\gamma\cos\gamma\right) + q\frac{\varpi}{e}\left(\frac{a_r e}{\varpi}\gamma + \cos\gamma - 1\right)\right\}.$$

We may get the potential for an internal point again by putting $\sin\gamma = e$. Therefore (4,5), (4,6), (4,7) and (4,9) give the forces and potential for any point $(\varpi,0)$ in the galactic plane.

We shall now consider an arbitrary point (ϖ,z) *off* the plane. The density is, by (2,10)

$$\rho = p + \frac{qe}{\sqrt{\varpi^2\sin^2\beta + z^2\operatorname{tg}^2\beta}}.$$

We need the integrals

$$\int \frac{\sin^2\beta\,d\beta}{\sqrt{\varpi^2\sin^2\beta + z^2\operatorname{tg}^2\beta}} = -\frac{1}{\varpi}\sqrt{\varpi^2\cos^2\beta + z^2},$$

$$\int \frac{\operatorname{tg}^2\beta\,d\beta}{\sqrt{\varpi^2\sin^2\beta + z^2\operatorname{tg}^2\beta}} = -\frac{1}{z}\ln\frac{\sqrt{\varpi^2\cos^2\beta + z^2} - z}{\varpi\cos\beta}.$$

From (2,21) and (2,22),

$$K_\varpi = 4\pi e^{-3}\sqrt{1-e^2}\,\varpi\left\{\tfrac{1}{2}p(\gamma-\sin\gamma\cos\gamma)+\frac{qe}{\varpi^2}\left(\sqrt{\varpi^2+z^2}-\sqrt{\varpi^2\cos^2\gamma+z^2}\right)\right\}, \tag{4,10}$$

$$K_z = 4\pi e^{-3}\sqrt{1-e^2}\,z\left\{p(\operatorname{tg}\gamma-\gamma)+\frac{qe}{z}\ln\frac{\left(\sqrt{\varpi^2+z^2}-z\right)\left(\sqrt{\varpi^2\cos^2\gamma+z^2}+z\right)}{\varpi^2\cos\gamma}\right\}, \tag{4,11}$$

where γ is given by

$$\sin\gamma = e \qquad \text{for internal points, or } a(\varpi,z)\leq a_r, \tag{4,12}$$

$$\varpi^2\sin^2\gamma + z^2\operatorname{tg}^2\gamma = a_r^2 e^2, \text{ for external points, or } a(\varpi,z) > a_r. \tag{4,13}$$

The potential at an external point is, by (2,23)

$$\Phi = 4\pi e^{-1}\sqrt{1-e^2}\left[p\int_0^{a_r}\beta a\,da + q\int_0^{a_r}\beta\,da\right]$$

$$= 4\pi e^{-1}\sqrt{1-e^2}\left[\tfrac{1}{2}pa_r^2\gamma + qa_r\gamma - \tfrac{1}{2}p\int_0^{\gamma}a^2 d\beta - q\int_0^{\gamma}a\,d\beta\right]$$

$$= 4\pi e^{-1}\sqrt{1-e^2}\left[\tfrac{1}{2}pa_r^2\gamma + qa_r\gamma - \frac{p}{2e^2}\int_0^{\gamma}(\varpi^2\sin^2\beta + z^2\operatorname{tg}^2\beta)\,d\beta - \frac{q}{e^2}\int_0^{\gamma}\sqrt{\varpi^2\sin^2\beta+z^2\operatorname{tg}^2\beta}\,d\beta\right]$$

$$= 4\pi e^{-3}\sqrt{1-e^2}\left[a_r e^2\gamma(\tfrac{1}{2}pa_r+q) - \tfrac{1}{2}p\left\{\tfrac{1}{2}\varpi^2(\gamma-\sin\gamma\cos\gamma)+z^2(\operatorname{tg}\gamma-\gamma)\right\}\right.$$

$$\left. - qe\left\{\sqrt{\varpi^2+z^2}-\sqrt{\varpi^2\cos^2\gamma+z^2}+z\ln\frac{\left(\sqrt{\varpi^2+z^2}-z\right)\left(\sqrt{\varpi^2\cos^2\gamma+z^2}+z\right)}{\varpi^2\cos\gamma}\right\}\right]. \tag{4,14}$$

According to (2,19) the potential for an internal point is the sum of (4,14) with a_r replaced by $a(\varpi,z)$ and γ by arc sin e, and a term

$$4\pi e^{-1}\sqrt{1-e^2}\arcsin e\int_{a(\varpi,z)}^{a_r}\left(p+\frac{q}{a}\right)a\,da = 4\pi e^{-1}\sqrt{1-e^2}\arcsin e\left\{\tfrac{1}{2}pa_r^2 - \tfrac{1}{2}pa^2(\varpi,z) + qa_r - qa(\varpi,z)\right\}.$$

Addition shows that the $a(\varpi,z)$ terms cancel, so that the potential of an internal point is obtained from (4,14) by replacing $\sin\gamma$ by e. Therefore, formulae (4,10) to (4,14) give the forces and potential for any point (ϖ,z) outside the galactic plane.

The mass of the non-homogeneous spheroid is

$$M = 4\pi\sqrt{1-e^2}\int_0^{a_r}\rho a^2\,da = 4\pi\sqrt{1-e^2}\,(\tfrac{1}{3}pa_r^3 + \tfrac{1}{2}qa_r^2). \tag{4,15}$$

5. *Observed quantities.*

With the aid of the formulae developed in section 4 we shall try to construct models of the distribution of mass. A few quantities relating to the Galactic System at large are known. We shall mention and discuss these quantities below.

(a) The circular velocities inside the sun in the galactic plane, the distance $\varpi_\circ$ of the sun to the galactic centre and the constants A and B of differential lactic rotation.

gaIt has been mentioned in section 3 that the rotational velocities of neutral hydrogen may be considered to be circular velocities. They were derived with the following assumed values of $\varpi_\circ$, A and B

$$\varpi_\circ = 8.2 \text{ kpc}, \tag{5,1}$$

$$A = 19.5 \text{ km/sec.kpc}, \tag{5,2}$$

$$B = -6.9 \text{ km/sec.kpc}, \tag{5,3}$$

where

$$A = \tfrac{1}{2}\left(\frac{\Theta_c}{\varpi} - \frac{\partial\Theta_c}{\partial\varpi}\right) = -\tfrac{1}{2}\varpi_\circ\frac{\partial\omega}{\partial\varpi},$$

$$B = -\tfrac{1}{2}\left(\frac{\Theta_c}{\varpi} + \frac{\partial\Theta_c}{\partial\varpi}\right).$$

We shall now discuss these values.

A direct determination of $\varpi_\odot$ has been attempted by BAADE [1]) from the magnitude distribution of RR Lyrae variables in a field near the galactic centre. He finds

$$\varpi_\odot = 8.2 \text{ kpc}. \qquad (5,4)$$

The values of the constants of galactic rotation A and B have been discussed by OORT [2]). His discussion was based on proper motions in the FK3 system. The same material was used by H. R. MORGAN and OORT [3]) to derive the rotation constants in the N30 system. The average values from the two systems are given as

$$A = +20 \text{ km/sec.kpc} \pm 2 \text{ (m.e.)}, \qquad (5,5)$$

$$B = -7 \text{ km/sec.kpc} \pm 1.5 \text{ (m.e.)}. \qquad (5,6)$$

The average of independent determinations of A from radial velocities is given as

$$A = +19 \text{ km/sec.kpc} \pm 2 \text{ (m.e.)}. \qquad (5,7)$$

Of more recent determinations we refer to articles by WEAVER and to a result derived by BLAAUW.

WEAVER [4]) determined the value of A from radial velocities of cepheid variables. He plotted the observed values of $\Delta\omega(\varpi) = \omega(\varpi) - \omega_\odot$ against ϖ. A value of

$$A = 10.8 \text{ km/sec. kpc}, \qquad (5,8)$$

with an estimated mean error of 1.8 km/sec.kpc, was obtained from the relation $A = -\frac{1}{2}\varpi_\odot \frac{\partial\omega}{\partial\varpi}$ by determining the slope of the $\Delta\omega(\varpi)$ curve at the sun's position. WEAVER admits that the material does not allow to draw a reliable curve for $\varpi < 7$ kpc. On the other hand the enormous spread of the points between $\varpi = 9$ and 10 kpc does not justify the way the smooth curve in his Figure 1c has been drawn for distances greater than $\varpi = 9$ kpc. Moreover, the curve drawn gives $\frac{\partial^2\omega}{\partial\varpi^2} < 0$. If most of the mass of the system is contributed by material less than, say, 5 kpc from the centre, the run of K_ϖ in the neighbourhood of the sun may be represented by $K_\varpi = \frac{\text{constant}}{\varpi^n}$, where $n > 0$. This will give $\frac{\partial^2\omega}{\partial\varpi^2} > 0$, however. Also none of the models, constructed and described in the present paper, yields a negative value of $\frac{\partial^2\omega}{\partial\varpi^2}$. Altogether it would seem that the form of WEAVER's curve $\Delta\omega(\varpi)$ should be considered with reserve. WEAVER relates the value of A to the local value of $\frac{\partial\omega}{\partial\varpi}$. This definition of A would give it a local meaning only. If the motions of cepheid variables show a very local irregularity, the exact value of $\frac{\partial\omega}{\partial\varpi}$ near the sun has little significance. An example may be found in *B.A.N.* No. 458, Figure 10, in which the ω values of the points between $\varpi = 7.5$ and 8.2 kpc lie considerably below the smooth $\omega(\varpi)$ curve; this deviation is probably due to local systematic motions of hydrogen clouds. WEAVER's definition of A as a purely local parameter thus does not seem satisfactory. Instead, it is to be preferred to determine the value of A from the slope of an $\omega(\varpi)$ curve, which stretches over a large range of ϖ. In this case it is possible to recognize and eliminate the effects of local irregularities. This would require a larger material with individually measured colour excesses.

In cases in which no individual distances are known, but only mean parallaxes, the evaluation of A is a difficult problem. A may then be obtained from the relation

$$\overline{V_r} = \bar{r} A \sin 2l', \qquad (5,9)$$

where V_r is the radial velocity and $l' = l - 327°.5$. If the material covers a large volume of space, the effect of local irregularities is probably averaged out. However, this involves a large range of distance, while (5,9) is an approximation which is sufficient only for small distances. The errors introduced by this procedure were discussed by WEAVER [5]), who calls the effect "mathematical bias". A valuable estimate of this bias, in so far as it is caused by the curvature of the $\omega(\varpi)$ curve, may be obtained by reducing the material separately in the two intervals $l = 57°$ — galactic anticentre — $237°$ and $l = 237°$ — galactic centre — $57°$. WEAVER calculates the expected bias in a number of examples, based on the form of his $\omega(\varpi)$ curve for cepheid variables. However the form of this curve does not seem well enough established, as discussed above, and the resulting values of the bias are likely to be much too high.

In a third paper WEAVER [6]) derived the value of A from radial velocities of B stars. For two thirds of the material luminosity classes were available. He found

$$A = 13.2 \text{ km/sec.kpc} \pm 2.7 \text{ (m.e.)}. \qquad (5,10)$$

It is difficult to judge in how far the above difficulties apply to this determination because the observational material has not been given.

---

[1]) Report of commission 33 of the I.A.U., *Draft Reports Dublin Meeting*, 285, 1955 and *Transactions of the I.A.U.*, Volume IX.

[2]) J. H. OORT, *Colloques Int. du Centre National de la Rech. Sc.* **25**, 60, 1950.

[3]) H. R. MORGAN and J. H. OORT, *B.A.N.* **11**, 379, 1951; No. 431.

[4]) H. WEAVER, *A.J.* **60**, 202, 1955.

[5]) H. WEAVER, *A.J.* **60**, 211, 1955.

[6]) H. WEAVER, *A.J.* **60**, 208, 1955.

BLAAUW [1]) determined A from distant B2 – B5 main-sequence stars. Mean luminosities of these stars were obtained from proper motions of relatively near stars. He used radial velocities and colours published by POPPER, and found

$$A = 20.0 \text{ km/sec.kpc} \pm 1.8. \qquad (5,11)$$

HINS and BLAAUW [2]) determined the axial ratio of the ellipsoidal velocity distribution of faint stars. The square of that ratio yields the following relation between A and B

$$\frac{-B}{A-B} = 0.24 \pm 0.04 \text{ (m.e.)}. \qquad (5,12)$$

The 21-cm observations finally furnish a most valuable check. The maximum radial velocities of neutral hydrogen observed in galactic longitudes $l = 15° - 30°$ at once determine the product $A\varpi_0$. The evaluation of this product as carried out in *B.A.N.* No. 452, page 133, is less satisfactory, however. In the first place the relation

$$V_{max} = 2A\varpi_0(1 - \sin l')\sin l' \qquad (5,13)$$

from which it was determined, is an approximate one. In the second place the method works only if the point on the line of sight, which is closest to the galactic centre, is situated in a region with considerable hydrogen density. Now a recent study [3]) of the distribution of neutral hydrogen in the inner parts of the system reveals that in the region $l = 15° - 30°$ this is only the case at about $l = 20°$. We shall therefore confine ourselves to this longitude. According to *B.A.N.* No. 458, Table 4, the observed maximum radial velocity at $l = 20°.9$ is $V_{max} = 52$ km/sec. The approximation (5,13) then yields

$$A\varpi_0 = 164 \text{ km/sec}. \qquad (5,14)$$

The exact formula is

$$V_{max} = \varpi_0(\omega - \omega_0)\sin l', \qquad (5,15)$$

or, neglecting third and higher order derivatives of ω,

$$V_{max} = \varpi_0 \sin l' \left\{(\varpi - \varpi_0)\frac{\partial\omega}{\partial\varpi} + \tfrac{1}{2}(\varpi - \varpi_0)^2\frac{\partial^2\omega}{\partial\varpi^2}\right\}$$

$$= \varpi_0 \sin l' \left\{-\varpi_0(1-\sin l')\frac{\partial\omega}{\partial\varpi} + \tfrac{1}{2}\varpi_0^2(1-\sin l')^2\frac{\partial^2\omega}{\partial\varpi^2}\right\}$$

$$= 2A\varpi_0 \sin l'(1-\sin l') + \tfrac{1}{2}\varpi_0^3 \sin l'(1-\sin l')^2\frac{\partial^2\omega}{\partial\varpi^2}. \qquad (5,16)$$

The second term, which gives the correction to (5,13), may be calculated by using the approximate relation

$$\omega = \sqrt{P + \frac{Q}{\varpi}}$$

found and discussed in section 3. This gives

$$\frac{\partial^2\omega}{\partial\varpi^2} = -\frac{2}{\varpi}\frac{\partial\omega}{\partial\varpi} - \frac{1}{\omega}\left(\frac{\partial\omega}{\partial\varpi}\right)^2,$$

from which we derive finally

$$V_{max} = 2A\varpi_0 \sin l'(1-\sin l')\left\{1 + (1-\sin l')\frac{-B}{\omega}\right\}. \qquad (5,17)$$

The correction term amounts to + 5% in the present case, so that the value of $A\varpi_0$ has to be decreased with 5%.

Hence $A\varpi_0 = 156$ km/sec. (5,18)

We have thus obtained finally relations (5,4), (5,5), (5,6), (5,7), (5,8), (5,10),(5,11), (5,12) and (5,18), from which should be decided at the best values of ϖ_0, A and B. It appears that the values (5,1), (5,2) and (5,3) agree satisfactorily with all the relations, except (5,8) and (5,10), which are due to WEAVER. Introduction of his values of A in relations (5,12) and (5,18) would yield values of B and ϖ_0, respectively, which deviate considerably from the other determinations of these quantities. The values (5,1), (5,2), (5,3), which have been used for the derivation of the rotational velocities and the structure of interstellar hydrogen, have also been used throughout the present work; there are some indications at present, that the value of A is a little too high. The angular velocity ω_0 near the sun is 26.4 km/sec.kpc and the circular velocity $\Theta_c = 216.5$ km/sec.

(b) The mass density near the sun.

The total density of mass near the sun should be not less than the sum of the masses of interstellar matter and known stars. The density of neutral interstellar hydrogen is estimated at 0.77 atoms/cm^3 or 1.28×10^{-24} gr/cm^3. The total hydrogen density is 1.42×10^{-24} gr/cm^3 if 10% is assumed to be ionized. The density of known stars [4]) is about 0.04 $\odot$/pc^3 or 2.7×10^{-24} gr/cm^3. Therefore the total mass density should be 4.2×10^{-24} gr/cm^3 at least.

(c) The distribution of neutral hydrogen.

From recent 21-cm surveys, which will soon be published in the *B.A.N.*, the most important features are given here. The density of neutral hydrogen in

[1]) A. BLAAUW, Report of Comm. 33 of the I.A.U., *Trans. I.A.U.* VIII, 505, 1954.
[2]) C. H. HINS and A. BLAAUW, *B.A.N.* **10**, 365, 1948; No. 391.
[3]) M. SCHMIDT, to be published in *B.A.N.*
[4]) A. BLAAUW, *Sterrekundig Colloquium Nederlandse Astronomen Club*, No. 9, 1951.

the galactic plane is about 0.4 atoms/cm^3 in the innermost regions ($\varpi < 3$ kpc). It rises to a value of 0.8 atoms/cm^3 at $\varpi = 7$ kpc, is about constant up to $\varpi = 10$ kpc and then decreases gradually until the density becomes zero at $\varpi = 15$ to 20 kpc. The thickness of the gas layer, defined as the distance between points where the density has dropped to half the density in the galactic plane, is 220 pc in the region of ϖ between 3 and 7 kpc. It may be supposed to have the same value near the sun.

(d) The force K_z near the sun.

The force K_z, perpendicular to the galactic plane, has been given by OORT [1]). The following values were read from Figure 4 of his paper:

$z =$ 0.1	0.2	0.3	0.4	kpc
$K_z =$ 1.7	3.4	3.8	3.9×10^{-9}	cm/sec^2.

After the present investigation was finished, a new determination of K_z by E. R. HILL became available, of which a short discussion will be given in section 12. A value of K_z at much higher values of z has been determined by OORT and VAN WOERKOM [2]), who found 8.4×10^{-9} cm/sec^2, with a probable error of 20%, for $z = 2 - 10$ kpc.

(e) Star densities.

Equidensity curves of faint stars, from counts at moderate and high galactic latitudes, within 1.5 kpc from the sun have been given by OORT [3]). These stars, which are mainly dwarf stars, contribute an important part to the mass density near the sun. Therefore the equidensity curves give an indication of how the surfaces of constant total mass density will run near the sun.

(f) The velocity of escape.

In galactic longitudes $l = 20° - 85°$ no apices of stars with velocities higher than 65 km/sec are found [4]). The limiting velocity may correspond to the velocity required to reach the boundary of the Galactic System, or it may correspond to the velocity of escape. In the last case the velocity of escape near the sun should be the sum of the circular velocity and 65 km/sec. In any case the velocity of escape near the sun should be 280 km/sec at least.

6. *Derived quantities.*

We shall obtain in this section some derived quantities which will be needed in the construction of models. It has been shown in section 3 that the run of the central force K_ϖ between $\varpi = 2.5$ and 8.2 kpc in the galactic plane may be represented approximately by

$$K_\varpi = P\varpi + Q. \qquad (6,1)$$

We shall choose the constants P and Q such, that the constants A and B of differential galactic rotation are reproduced. By (6,1)

$$\omega = \sqrt{\frac{K_\varpi}{\varpi}} = \sqrt{P + \frac{Q}{\varpi}},$$

$$\frac{\partial \omega}{\partial \varpi} = -\frac{Q}{2\varpi^2 \omega},$$

so $$A = \frac{Q}{4\varpi\,\omega},$$

or $$Q = 4\varpi\,\omega A. \qquad (6,2)$$

Further $$P = \omega^2 - \frac{Q}{\varpi},$$

$$= \omega(\omega - 4A). \qquad (6,3)$$

We now substitute the values of A and B decided upon in the previous section,

$$A = +\ 19.5 \text{ km/sec.kpc},$$

$$\omega = A - B = +\ 26.4 \text{ km/sec.kpc},$$

from which $$P = -\ 1362 \text{ km}^2/\text{sec}^2.\text{kpc}^2, \qquad (6,4)$$

$$Q = +\ 16885 \text{ km}^2/\text{sec}^2.\text{kpc}. \qquad (6,5)$$

These values were used in section 3 to compare the assumed force law (3,2) with the observations. The representation was quite satisfactory. The values of P and Q given above reproduce at the same time the observed values of A and B and approximately the run of K_ϖ between $\varpi = 2.5$ kpc and 8.2 kpc as derived from the 21-cm measures.

A second derived quantity is the mass density $\rho_\circ$ near the sun. This may be determined by Poisson's equation from K_z for small z values, and A and B,

$$\frac{\partial K_\varpi}{\partial \varpi} + \frac{K_\varpi}{\varpi} + \frac{\partial K_z}{\partial z} = 4\pi\rho_\circ.$$

Now $$\frac{\partial K_\varpi}{\partial \varpi} = -(A - B)(3A + B),$$

$$\frac{K_\varpi}{\varpi} = \quad (A - B)^2,$$

and from section 5d

$$\frac{\partial K_z}{\partial z} = 17 \times 10^{-9} \text{ cm/sec}^2.\text{kpc or}$$

5250 km^2/sec^2.kpc^2, so that the density in mass units (cf. section 1) is

$$\rho_\circ = 365 \text{ or } 5.76 \times 10^{-24} \text{ gr/cm}^3 \text{ or } 0.085\ \odot/\text{pc}^3.$$

---

[1]) J. H. OORT, *B.A.N.* **6**, 249, 1932; No. 238.
[2]) J. H. OORT and A. J. J. VAN WOERKOM, *B.A.N.* **9**, 185, 1941; No. 338.
[3]) J. H. OORT, *B.A.N.* **8**, 233, 1938; No. 308.
[4]) J. H. OORT, *B.A.N.* **4**, 269, 1928; No. 159.

It should be noted that this value of ρ_0 is not very certain, because the value of K_z at small z values is not yet known with great accuracy.

The values of the derived quantities P, Q and ρ_0 used in the model calculations differ a little for different models. The values actually used for each model are given in the relevant sections.

7. *First model of the mass distribution.*

We shall now derive a first, simple model of the distribution of mass in the Galactic System. For the construction of this model the following values of the derived constants were used

$$P = -1350,\ Q = 16760,\ \rho_0 = 358.$$

If we suppose the sun to be inside the spheroid, we have by (4,2) and (4,3) the following equations

$$p + \frac{q}{8.2} = 358,$$

$$2\pi e^{-3}\sqrt{1-e^2}\,(\arcsin e - e\sqrt{1-e^2})\,p = -1350,$$

$$4\pi e^{-2}\sqrt{1-e^2}\,(1 - \sqrt{1-e^2})\,q = 16760,$$

from which

$$p = -2126,\ q = 20365,\ \sqrt{1-e^2} = \frac{c}{a} = 0.07. \quad (7,1)$$

By (4,4) $a_r = 9.58$,

so that the sun is indeed situated inside the spheroid. The present extremely simple model may be considered as representing a mean distribution of mass yielding a correct density near the sun and the approximate force law in the plane. The value 0.07 for the axial ratio agrees well with the value of $\frac{1}{12}$ which WYSE and MAYALL [1]) found from the distribution of light in a number of edge-on spiral nebulae. The logarithmic density gradient $\frac{\partial \log \rho}{\partial \varpi}$ near the sun is

$$\frac{\partial \log \rho}{\partial \varpi} = \frac{\mathrm{Mod}}{\rho_0} \cdot \frac{-q}{{\varpi_0}^2} = -0.053\,\frac{a_r}{a_r - 8.2}, \quad (7,2)$$

or -0.37 for the present model. This is an extremely high value, higher than of any known type of objects in the Galactic System. With the density law used this gradient depends only on a_r. It may easily be seen that the greatest possible value of a_r occurs in the case of a flat disc, i.e. for $e = 1$, in which case $a_r = -\frac{\pi}{4}\frac{Q}{P}$, corresponding to $\frac{\partial \log \rho}{\partial \varpi} = -0.33$, a value only slightly lower than the one found above. This large mass-density gradient recurs as an important feature in all subsequent models. It shows that an important part of the mass of the Galactic System must be due to unknown objects with a large logarithmic density gradient near the sun. This feature had already been found by OORT [2]). By Newton's theorem only the mass within a spheroid with $a = 8.2$ kpc and $\frac{c}{a} = 0.07$ will contribute to the forces within the sun's distance from the centre. Provided we keep e unchanged, we may therefore replace, in shells outside the sun, the density law $\rho = p + \frac{q}{a}$ by any other density law without influencing the circular velocities inside ϖ_0. It appeared that for $a > 8.2$ a density law of the form

$$\rho = \frac{s}{a^4} \quad (7,3)$$

would give the best representation of the density of faint stars at high galactic latitudes (cf. section 5e). The density at $\varpi = 8.2$, $z = 0$ was 358, so $s = 358 \times 8.2^4$. Mathematically the shell may be considered as the difference of two spheroids. The shell in this case is the difference between a spheroid with $a_r = \infty$ and a spheroid with $a_r = 8.2$. By (2,15) and (2,21) we have for a point in the shell in the galactic plane

$$K_{\varpi_{sh}} = 4\pi e^{-3}\sqrt{1-e^2}\,\varpi \int_{\gamma}^{\arcsin e} \frac{s}{a^4}\sin^2\beta\, d\beta,$$

with $\sin\beta = \frac{ae}{\varpi}$ and $\sin\gamma = \frac{8.2e}{\varpi}$.

Hence

$$K_{\varpi_{sh}} = 4\pi e\sqrt{1-e^2}\,\frac{s}{\varpi^3}\left(\frac{\sqrt{\varpi^2 - (8.2e)^2}}{8.2e} - \frac{\sqrt{1-e^2}}{e}\right). \quad (7,4)$$

The total force K_ϖ in a point $\varpi > 8.2$, $z = 0$ then is the sum of the force (4,5) due to the spheroid (7,1) up to a limiting surface with $a_r = 8.2$, and the force (7,4) due to the shell. The forces thus computed are given in Table 6 together with the corresponding circular velocities; the latter are also shown in Figure 2.

The mass of the system is the sum of the mass of the spheroid with $a_r = 8.2$, (4,15), and the mass of the shell, which is $4\pi\sqrt{1-e^2}\,\frac{s}{8.2}$. We find $M_{sph} = 257800$ and $M_{sh} = 173600$, so that, in total,

$$M = 431400, \text{ or } 1.01 \times 10^{11}\odot.$$

It will be clear from what has been mentioned above about the shell, that its mass is quite uncertain.

[1]) *Loc. cit.*

[2]) J. H. OORT, *Ap. J.* **116**, p. 238–239, 1952.

It does not seem worth while to compute more properties of the present model. It does not properly take account of the known differences in concentration towards the galactic plane and towards the galactic centre as observed for different types of objects, and can therefore be regarded only as a first attempt.

8. *Second model of the mass distribution.*

We shall now describe a second model of the mass distribution. This model has been considered for some time as being the best possible one at present and the resulting curve of rotational velocities outside the sun has been used for the reduction of the Dutch 21-cm observations of 1954–1955. It has now been superseded by another model which will be described in section 9. Still it seems worth while to describe the model, in order to carry out comparisons afterwards.

It consists of three non-homogeneous spheroids, the first one representing population I objects, the second one F—M stars and the third one other, unknown objects. A major difficulty presents itself at once: what is the density law for these different types of objects? Our knowledge is restricted to values of the density gradient near the sun which, moreover, are not very accurate. It has been assumed that the density of each type of object can be represented as $\rho = p + \frac{q}{a}$. Each spheroid then gives a force of the form $K_\varpi = P\varpi + Q$, and the total force will have the same form, as required. It is realized, however, that this density law is not much more than a guess for those types of objects which contribute little to the total mass of the system.

The density of population I objects may be estimated as follows. The average hydrogen density near the sun (cf. section 5b) is 1.42×10^{-24} gr/cm^3. The density of O, B and A stars is 0.0022 $\odot$/pc^3 or 0.15×10^{-24} gr/cm^3. Accordingly, the total density near the sun has been taken as 100 mass units. A study [1]) of the z-distribution of neutral hydrogen gave a density of 50% of the density in the plane at $z = 115$ pc and 13% at 230 pc. With a density law

$$\rho_1 = p_1 + \frac{q_1}{\sqrt{\varpi^2 + \frac{z^2}{1 - e_1^2}}},$$

it appears possible to choose the parameters p_1, q_1, and e_1, such that these relative densities are represented. We get

$$p_1 = -45, \quad q_1 = 1190, \quad \frac{c_1}{a_1} = \sqrt{1 - e_1^2} = 0.0122,$$

so $$\rho_1 = -45 + \frac{1190}{a_1}, \quad a_{r_1} = 26.4 \text{ kpc},$$

and $$K_{\varpi_1} = -5.3\varpi + 180. \tag{8,1}$$

The following values of the derived quantities were used in this model,

$$P = -1362, \quad Q = 16890, \quad \rho_\odot = 358.$$

Now from (8.1), $P_1 = -5.3$, $Q_1 = 180$,

so

$$P_2 + P_3 = -1356.7, \; Q_2 + Q_3 = 16710. \tag{8,2}$$

The density of the first spheroid near the sun is 100, so

$$p_2 + p_3 + \frac{q_2 + q_3}{8.2} = 258. \tag{8,3}$$

We shall take a logarithmic density gradient in the second spheroid near the sun of -0.10, from which, by (7,2)

$$a_{r_2} = -\frac{q_2}{p_2} = 17.4. \tag{8,4}$$

It appears from *B.A.N.* No. 308, Figure 8, that the star density has decreased to 50% at $z = 350$ pc about, so

$$\tfrac{1}{2}\left(p_2 + \frac{q_2}{8.2}\right) = p_2 + \frac{q_2}{\sqrt{8.2^2 + \frac{0.35^2}{1 - e_2^2}}}. \tag{8,5}$$

At the time this model was constructed it was believed that the third spheroid consisted mainly of high-velocity objects and consequently would not be very flat. A value of

$$\frac{c_3}{a_3} = \sqrt{1 - e_3^2} = 0.30 \tag{8,6}$$

was assumed. We have then sufficient data to solve for all the unknowns. Equations (8,2)—(8,6) give the following set of spheroids

$$\left.\begin{array}{llllll} \sqrt{1 - e_1^2} = 0.0122 & , \; \rho_1 = -45 + \dfrac{1190}{a_1} & , \; a_{r_1} = 26.4 & , \; \rho_{10} = 100 & . \\ \sqrt{1 - e_2^2} = 0.05 & , \; \rho_2 = -214 + \dfrac{3720}{a_2} & , \; a_{r_2} = 17.4 & , \; \rho_{20} = 240 & . \\ \sqrt{1 - e_3^2} = 0.30 & , \; \rho_3 = -591 + \dfrac{4997}{a_3} & , \; a_{r_3} = 8.46 & , \; \rho_{30} = 18 & . \end{array}\right\} \tag{8,7}$$

The logarithmic density gradient near the sun is in the third spheroid

$$\frac{\partial \log \rho_3}{\partial \varpi} = -1.79.$$

The density at $\varpi = 7.2$ is not 52 times the density near the sun, as the gradient would suggest, but 5.7 times, which still is very much. On the other hand it is very unsatisfactory that only 260 pc outside the sun the density in the third ellipsoid has dropped to zero already. This may be improved by replacing the

[1]) M. SCHMIDT, *loc. cit.*

spheroid for $a > 8.2$ by a shell with a different density law. We shall use for $a > 8.2$

$$\rho_{sh} = \frac{w}{a^4 - m^4} , \qquad (8,8)$$

in which the values of w and m are chosen such that the density and the density gradient are continuous at the transition from spheroid to shell.

This gives $$\rho_{sh} = \frac{10000}{a^4 - 3965} \text{ for } a > 8.2. \qquad (8.9)$$

The shell has the same axial ratio as the third spheroid. The force K_ϖ in the galactic plane, due to such a shell, is

$$K_{\varpi_{sh}} = \frac{2\pi w E}{m^2 \varpi}\left\{\frac{1}{S}\left(\operatorname{arc\,tg}\frac{D}{S} - \operatorname{arc\,tg}\frac{E}{S}\right) + \frac{1}{2V}\ln\frac{(V+D)(V-E)}{(V-D)(V+E)}\right\}, \qquad (8,10)$$

where

$$E = \frac{1}{e}\sqrt{1-e^2}\ , \quad D = \frac{\varpi}{8.2\,e}\sqrt{1-\left(\frac{8.2\,e}{\varpi}\right)^2},$$

$$S = \sqrt{1+\left(\frac{\varpi}{me}\right)^2}, \quad V = \sqrt{-1+\left(\frac{\varpi}{me}\right)^2}.$$

The total force K_ϖ outside the sun in the galactic plane is the sum of the forces due to the spheroids (8,7), which may be computed from (4,5) with $a_{r_3} = 8.2$, and the force (8,10) due to the shell (8.9). The forces thus computed are given in Table 6 together with the corresponding circular velocities, which are also shown in Figure 2.

The masses of the spheroids may be computed from (4,15), with $a_{r_3} = 8.2$. The mass of the shell is

$$M_{sh} = 2\pi\sqrt{1-e^2}\,\frac{w}{m}\left\{\frac{\pi}{2} - \tfrac{1}{2}\ln\frac{8.2-m}{8.2+m} - \operatorname{arc\,tg}\frac{8.2}{m}\right\}.$$

The masses are $M_1 = 21300$, $M_2 = 119000$, $M_3 = 224000$, $M_{sh} = 6900$,

so in total $M = 371000$, or $0.86 \times 10^{11}\,\odot$.
Some of the less satisfying properties of the present model will be mentioned and discussed in the following section.

9. *Third model of the mass distribution.*

In this section an improved model of the mass distribution will be given. It consists of four non-homogeneous spheroids, each of which has a density law $\rho = p + \frac{q}{a}$.

The first spheroid, which again represents population I objects, reached to a distance of 26.4 kpc in the previous model. The results of a recent survey [1]) of neutral hydrogen near the galactic plane at 21-cm wave length show however that at about $\varpi = 12\frac{1}{2}$ kpc the density of neutral hydrogen has dropped to one third of the density near the sun. We maintain $\rho_{10} = 100$ so that then

$$\rho_1 = -100 + \frac{1640}{a_1} \qquad (9,1)$$

and $a_{r_1} = 16.4$ kpc, which is much more reasonable. Now the eccentricity e_1 is chosen such as to get the best fit with the observed z-distribution of neutral hydrogen. The fit is quite satisfactory for

$$\frac{c_1}{a_1} = \sqrt{1-e_1^2} = 0.02. \qquad (9,2)$$

The density of neutral hydrogen in the inner parts of the system, as given in section 5c, is rather lower than given by (9,1). The contribution of the first spheroid to the forces in the inner parts is minor and it may easily be calculated that the deviations have a negligeable influence. The first spheroid is completely defined now.

The second spheroid will again consist of F – M stars. We shall try to represent the equidensity curves shown in *B.A.N.* No. 308, Figure 8, as accurately as possible. After slightly smoothing the curves shown, we get the following densities above the sun expressed in the density at $z = 0$,

$z = 0$	0.45	0.67	1.2 kpc
$\rho = 1$	0.41	0.16	0.04

The logarithmic density gradients at $z = 1040$ pc and 1410 pc are given as -0.13 and -0.15, respectively. From the figure a value of -0.20 may be found at $z = 600$ pc. We shall assume a value $\frac{\partial \log \rho_2}{\partial \varpi} = -0.16$ in the galactic plane. Then, by (7,2), $a_{r_2} = 12.3$ kpc. Now by (4,2) and (4,4) the density may be written as $\rho_2 = p_2\left(1 - \frac{12.3}{a_2}\right)$, where $a_2 = \sqrt{\varpi^2 + \frac{z^2}{1-e_2^2}}$. Therefore each relative density at a z-level gives a determination of e_2. Now the relative densities at $z = 0.45$ and 0.67 kpc are represented reasonably well with $\frac{c_2}{a_2} = \sqrt{1-e_2^2} = 0.078$, but with this axial ratio the spheroid reaches no further than $z = 0.72$ kpc, so that the density at $z = 1.2$ kpc cannot be represented.

In order to overcome this difficulty it seems best to introduce a third spheroid representing the stars with the higher z-velocities. This makes it possible to rep-

[1]) To be published in *B.A.N.*

resent also the slope of the equidensity curves, which at $z = 1.2$ kpc is 10°. This fixes at once the axial ratio of the third spheroid, because $\text{tg } 10° = \frac{8.2}{1.2}(1 - e_3^2)$;

we thus obtain $\frac{c_3}{a_3} = \sqrt{1 - e_3^2} = 0.16.$ (9,3)

We assume a star density near the sun of $0.042_5 \odot/\text{pc}^3$ (cf. section 5b); therefore

$$\rho_{20} + \rho_{30} = 185.$$

The star density at $z = 1.2$ kpc is then 7.4 units. Assuming the same logarithmic density gradient as in the second spheroid, it is then possible to calculate p_3 and q_3, and we get

$$\rho_3 = -70 + \frac{861}{a_3}, \qquad (9,4)$$

so that $\rho_{30} = 35$ and $\rho_{20} = 150$. After subtraction of the part due to the third spheroid, the relative star densities at $z = 0.45$ and 0.67 kpc may be represented satisfactorily by taking an axial ratio of the second

spheroid $\frac{c_2}{a_2} = \sqrt{1 - e_2^2} = 0.07,$ (9,5)

while from $a_{r_2} = 12.3$, $\rho_{20} = 150$,

$$\rho_2 = -300 + \frac{3690}{a_2}. \qquad (9,6)$$

This completes the description of three spheroids. For each of the spheroids the force law for $\varpi < 8.2$, $z = 0$ is easily computed. We get in total

$$K_{\varpi_1} + K_{\varpi_2} + K_{\varpi_3} = -301.4\,\varpi + 4938.$$

The total force is given by

$$K_\varpi = -1362\,\varpi + 16885,$$

the constants of which have been derived in section 6. The excess force observed has to be attributed to unknown objects, because no objects are known, other than those already represented, which would contribute enough to explain such a large force excess. We can do not much better than putting these unknown objects in one non-homogeneous spheroid. The force due to this spheroid then is

$$K_{\varpi_4} = -1060.6\,\varpi + 11947.$$

The density near the sun in this spheroid is $\rho_\circ - (\rho_{10} + \rho_{20} + \rho_{30})$, if $\rho_\circ$ is the total density. The value of $\rho_\circ$ is taken a little higher than before, viz. $\rho_\circ = 383$ or 6.04×10^{-24} gr/cm^3.
Therefore $\rho_{40} = 98$, and the axial ratio of the fourth spheroid becomes

$$\frac{c_4}{a_4} = \sqrt{1 - e_4^2} = 0.07, \qquad (9,7)$$

while $$\rho_4 = -1670 + \frac{14499}{a_4}. \qquad (9,8)$$

The boundary of the fourth spheroid is at $a_{r_4} = 8.68$ kpc and the logarithmic density gradient near the sun is

$$\frac{\partial \log \rho_4}{\partial \varpi} = -0.95.$$

The gradient is high again, although rather less than in the preceding model. The density at $\varpi = 7.2$ kpc is not 9 times the density near the sun, as the gradient would suggest, but only 3.5 times. On the other hand, the density in the fourth spheroid drops to zero at a distance of only 480 pc from the sun. The outer parts of the spheroid have not been replaced by a shell in the present model, mainly because such a shell cannot be founded on any observations.

The present model will be discussed further in section 12.

10. *Estimates of velocity dispersions.*

A model of the distribution of mass should approximately satisfy conditions of equilibrium. In a dynamically steady state the equation of continuity yields the following relations [1]) for a system with axial symmetry:

$$\frac{\partial(\rho\sigma_\Pi^2)}{\partial\varpi} + \frac{\rho}{\varpi}(\sigma_\Pi^2 - \overline{\Theta^2}) = -\rho K_\varpi, \qquad (10,1)$$

$$\frac{\partial(\rho\sigma_Z^2)}{\partial z} = -\rho K_z, \qquad (10,2)$$

with $$\sigma_\Pi^2 = \sigma_Z^2, \qquad (10,3)$$

where $\sigma_\Pi^2 = \overline{\Pi^2}$ and $\sigma_Z^2 = \overline{Z^2}$ are the mean square velocity components parallel to the ϖ-axis and the z-axis, respectively; $\overline{\Theta^2}$ is the mean square component perpendicular to the other two. All velocities are relative to the centre of the Galactic System. The component $\overline{\Theta^2}$ may be separated in two terms,

$$\overline{\Theta^2} = \bar{\Theta}^2 + \sigma_\Theta^2. \qquad (10,4)$$

It is known that for most objects equation (10,3) is not fulfilled. Near the sun σ_Π is generally about 1.5 to 2 times σ_Z. This shows that the system has not yet attained a state of strict equilibrium, which may be due to a not complete conversion of average Π motions into Z motions and vice versa [2]).

We shall use relations (10,1) and (10,2) to investigate the velocity dispersions in the mass models. By integrating (10,2) we get

$$\rho\sigma_Z^2 = \int_z^\infty \rho K_z dz, \qquad (10,5)$$

so that σ_Z may be determined for any mass model. Now let

$$\sigma_\Pi = \mu\sigma_Z. \qquad (10,6)$$

[1]) J. H. JEANS, *M.N.* **82**, 123, 1922.
[2]) J. H. OORT, *B.A.N.* **4**, 269, 1928; No. 159.

It is then possible, with some assumed value of μ, to calculate $\overline{\Theta^2}$ from (10,1). It is impossible generally to get $\overline{\Theta}$ and σ_Θ separately. Near the sun however, many objects fulfill STRÖMBERG's [1]) empirical relation between σ_Θ and the rotational velocity near the sun $\overline{\Theta}_\circ$,

$$\overline{\Theta}_\circ - \Theta_c = -0.0192\,\sigma_\Theta^2 , \qquad (10,7)$$

all velocities being expressed in km/sec. STRÖMBERG gave an additional constant in his original relation, which may be dropped here. Equations (10,4) and (10,7) enable one to separate the rotational velocity $\overline{\Theta}_\circ$ and the velocity dispersion σ_Θ near the sun. It may very well be that unknown objects do not obey STRÖMBERG's relation. In that case no separation can be made.

We first investigate the third spheroid of the second model (section 8) which consists of unknown objects. The dispersion of Z velocities near the sun is found to be $\sigma_Z = 35$ km/sec. From (10,1) and (10,6) we find near the sun, $\overline{\Theta^2} = 48100 - 41000\,\mu^2$. If II and Z dispersions are equal, $\mu = 1$ and $\overline{\Theta^2} = 7100$ km^2/sec^2. If $\sigma_\Theta = \sigma_{II} = 35$ km/sec, the rotational velocity near the sun would be $\overline{\Theta}_\circ = 77$ km/sec. A combination of $\overline{\Theta}_\circ$ and σ_Θ like this has not been observed for any type of objects in the system. Moreover, if $\mu > 1.09$, $\overline{\Theta^2}$ becomes negative and the mass spheroid cannot exist at all. It seems improbable that the third spheroid of the second model represents a possible distribution of mass, although the possibility that the unknown objects should have a velocity distribution entirely different from the distributions observed, cannot be ruled out altogether.

The failure of the second model is due to the high logarithmic density gradient in the third spheroid. It does not seem possible to escape a large gradient, and the only possibility of limiting its influence in (10,1) is to reduce σ_{II}. This implies a reduction of σ_Z and consequently a distribution of mass with a stronger concentration to the galactic plane. In general, high-velocity objects combine a larger logarithmic density gradient in the plane with a more nearly spherical distribution in the Galactic System. Here, however, we find that a very large logarithmic density gradient must be accompanied by a rather flat distribution, in order to satisfy conditions of equilibrium and continuity. Such a distribution would be like that of the disc population II objects which are such a striking feature of the Andromeda nebula.

In this connection the flat form of the fourth spheroid of the third model (section 9) seems much more favourable. It should be noted that the parameters of this spheroid were not chosen freely, but were entirely determined by the remaining parts of the force law and the density near the sun.

Table 2 gives for both the third and fourth spheroids of the third model computed values of σ_Z and $\overline{\Theta^2}$ for a number of points in the galactic plane. The third spheroid consisted of F–M stars with high Z velocities.

TABLE 2

Values of σ_Z and $\overline{\Theta^2}$ in the galactic plane for the third and fourth spheroids of the third mass model (section 9). The ratio of σ_{II} and σ_Z is μ.

	Third spheroid		Fourth spheroid	
ϖ kpc	σ_Z km/sec	$\overline{\Theta^2}$ km^2/sec^2	σ_Z km/sec	$\overline{\Theta^2}$ km^2/sec^2
2.05	91	$28880 - 3220\,\mu^2$	47	$28880 - 2310\,\mu^2$
4.10	78	$46330 - 8870\,\mu^2$	36	$46330 - 4050\,\mu^2$
6.15	56	$52340 - 10980\,\mu^2$	22	$52340 - 4390\,\mu^2$
8.20	34	$46880 - 7850\,\mu^2$	7(10)	$46880 - 2720\,\mu^2$
10.25	18	$29970 - 4080\,\mu^2$		

The dispersion of Z velocities near the sun is $\sigma_Z = 34$ km/sec. It is possible to satisfy STRÖMBERG's relation for $\mu = 1.7$, which is a reasonable value. We then get near the sun

$$\overline{\Theta}_\circ = 142 \text{ km/sec}, \quad \sigma_{II} = \sigma_\Theta = 60 \text{ km/sec}.$$

This shows that the third spheroid represents a possible mass distribution.

The fourth spheroid consists of unknown objects. The Z dispersion near the sun is only 7 km/sec. We shall assume a somewhat higher value, because it may be expected that the density towards higher z values decreases somewhat more slowly than given by the spheroid. It may be expected that the Z dispersion near the sun is appreciably smaller than at $\varpi = 6.15$ kpc and we assume $\sigma_Z = 10$ km/sec, as indicated in parentheses in Table 2. The resulting value of $\overline{\Theta^2}$ near the sun is $\overline{\Theta^2} = 46880 - 2720\,\mu^2$. Now, $\overline{\Theta^2}$ is positive for a large range of μ. This is much more favourable than in the second mass model discussed above. A separation of $\overline{\Theta^2}$ is not possible because it is not at all certain that the objects obey STRÖMBERG's relation. Altogether the third mass model is to be preferred to the second model.

The velocity dispersions given in Table 2 are useful to get an impression of the run of the dispersions throughout the system. The value of μ will probably be different at different positions in the system. Once the values of μ are known, it is possible to calculate the velocity dispersions of the unknown objects everywhere in the system.

If a model is to be entirely satisfactory it should specify not only the velocity dispersions, but the complete velocity distribution of the objects of which it consists, and it should be proved that these velocity

[1]) G. STRÖMBERG, *Ap. J.* **61**, 379, 1925.

distributions are consistent with the density distributions and potentials assumed. This rather more difficult phase of model investigation was considered to be beyond the scope of the present investigation.

11. *The deviations from the assumed force law.*

Up to now we have entirely neglected the differences between the forces observed in the galactic plane and the forces computed by (3,2), as given in Table 1. These differences are not large and can easily be taken into account by adding a system of homogeneous spheroids. A set of 9 homogeneous spheroids was added for this purpose, each with an axial ratio of 0.07, this being about the mean axial ratio of the whole system. The densities of the spheroids are taken such that the force differences given in Table 1 are represented as well as possible. The densities of these homogeneous spheroids are given in Table 4 of the following section. Near the sun the density due to these spheroids is about + 19, which is a minor fraction of the total density. For larger distances from the centre, in the galactic plane, the force K_ϖ due to the homogeneous spheroids is given in Table 3.

TABLE 3

Forces K_ϖ in the galactic plane due to the homogeneous spheroids

ϖ kpc	K_ϖ km²/sec².kpc
9	− 28
10	− 27
12	− 19
15	− 11
20	− 8

It is seen to be very small. The total mass of the set of homogeneous spheroids is − 3000, which is only − 1% of the mass of the Galactic System.

TABLE 4

Parameters and properties of the final model

Non-homogeneous spheroids				
Spheroid	1	2	3	4
Objects	population I	F−M stars	high-velocity F−M stars	unknown objects
$c/a = \sqrt{1-e^2}$	0.02	0.07	0.16	0.07
a_r	16.4	12.3	12.3	8.68
c_r	0.33	0.86	1.97	0.61
$z_r(\varpi = 8.2)$	0.28	0.64	1.47	0.20
ρ	$-100 + \frac{1640}{a}$	$-300 + \frac{3690}{a}$	$-70 + \frac{861}{a}$	$-1670 + \frac{14499}{a}$
$a(\varpi,z)$	$\sqrt{\varpi^2 + 2500\,z^2}$	$\sqrt{\varpi^2 + 204\,z^2}$	$\sqrt{\varpi^2 + 39\,z^2}$	$\sqrt{\varpi^2 + 204\,z^2}$
ρ_0	100	150	35	98
$\frac{\partial \log \rho_0}{\partial \varpi_0}$	− 0.05	− 0.16	− 0.16	− 0.95
M	18500	81800	43600	160300

Homogeneous spheroids									
Axial ratio c/a	all 0.07								
a	0.84	1.90	2.93	3.90	5.09	6.13	7.16	8.10	8.20
ρ	+ 27000	+ 608	+ 99	− 113	− 199	− 69	+ 1	+ 9	+ 20
M	− 3000 in total								

12. *Forces and potentials in the final model.*

We shall in this section consider the final model, which consists of the four non-homogeneous spheroids of the third model (section 9) and a set of nine homogeneous spheroids (section 11). A general review of parameters and properties of all the spheroids is given in Table 4. The value of z corresponding to the boundary of each of the non-homogeneous spheroids, at the sun's distance from the galactic centre, is given as $z_r(\varpi = 8.2)$. The density at a point (ϖ,z) in a spheroid is obtained by substituting $a(\varpi,z)$ in the formula for the density. The total density at any point is the sum of the densities of all the spheroids which contain the point considered. Total mass densities for

a number of points are given in Table 5. A diagram of the mass density in the (ϖ,z)-plane, expressed in the density near the sun as a unit, is given in Figure 1. The total density near the sun in the present model is 402, or 6.34×10^{-24} gr/cm^3, or 0.093 $\odot$/pc^3. The total mass of the system is 301200 or 1.395×10^{44} gr or $0.702 \times 10^{11}\,\odot$. The force K_ϖ has been calculated for a number of points with $\varpi > \varpi_c$ in the galactic plane. The corresponding circular and angular velocities are given in Table 6 together with the values obtained in the first and second mass models. The circular velocities are also shown in Figure 2. For $\varpi < 8.2$ kpc the first and second models give a rotation curve $\Theta_c = \varpi \sqrt{P + \frac{Q}{\varpi}}$, while the final model gives an accurate representation of the observed circular velocities.

Calculations of the potential Φ and the forces K_ϖ and K_z were carried out for a number of z-values at $\varpi = 0$, 2.05, 4.10, 6.15, 8.20, 10.25, 12.30 and 16.40 kpc. At intermediate values of ϖ and z, Φ, K_ϖ and K_z were determined by graphical interpolation.

Due to this procedure small errors may have been introduced, but it has been tried to make the potentials and forces consistent. The results are given in Tables 7, 8 and 9, and are shown graphically in Figures 3, 4 and 5.

TABLE 5

Total mass densities in 10^{-24} gr/cm^3.

ϖ (kpc)	0	2.05	4.10	6.15	8.20	10.25	12.30
z (kpc)							
0		123	40.9	19.6	6.34	2.11	0.52
0.1	200	88	35.0	17.4	5.29	1.78	0.38
0.2	76	50	26.5	13.4	2.97	1.18	0.06
0.3	38.3	30.3	18.9	8.8	2.07	0.69	
0.4	22.9	18.5	11.8	4.1	1.58	0.41	
0.5	12.8	10.4	5.7	2.29	1.04	0.16	
0.6	4.9	4.6	2.75	1.59	0.58	0.14	
0.7	3.09	2.67	1.81	0.92	0.37	0.11	
0.8	1.97	1.58	0.99	0.62	0.33	0.08	
0.9	1.31	1.10	0.84	0.52	0.28	0.05	
1.0	1.07	0.93	0.71	0.44	0.23	0.02	
1.2	0.71	0.63	0.49	0.30	0.14		
1.4	0.44	0.41	0.30	0.16	0.04		
1.6	0.25	0.22	0.16	0.06			
1.8	0.09	0.08	0.05				

FIGURE 1

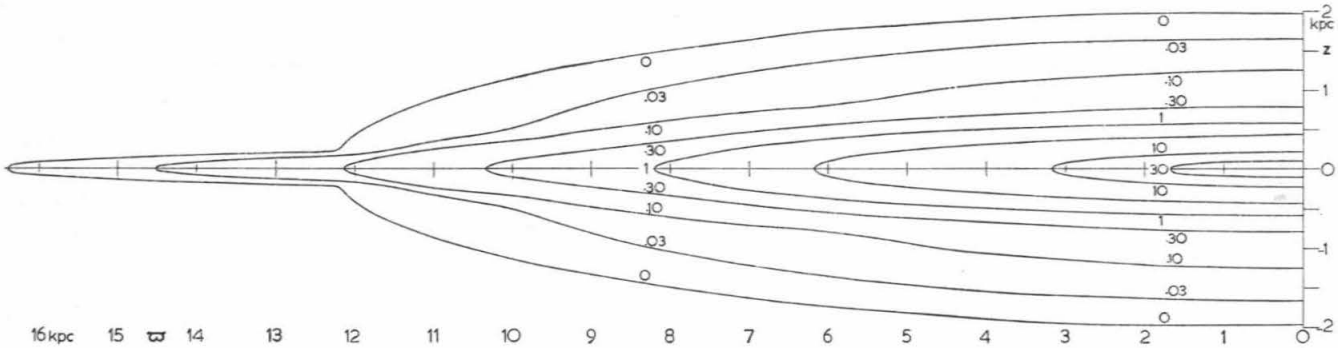

Total mass densities in the (ϖ,z)-plane, expressed in the density near the sun as a unit.

TABLE 6

Forces and velocities in the outer parts of the galactic plane for three models.

	Model 1			Model 2			Final model		
ϖ kpc	K_ϖ km^2/sec^2.kpc	Θ_c km/sec	ω km/sec.kpc	K_ϖ km^2/sec^2.kpc	Θ_c km/sec	ω km/sec.kpc	K_ϖ km^2/sec^2.kpc	Θ_c km/sec	ω km/sec.kpc
8.2	56.9	216	26.4	57.2	216	26.4	57.2	216	26.4
9	48.0	208	23.1	47.7	207	23.0	46.8	205	22.8
10	39.6	199	19.9	39.4	198	19.8	37.9	195	19.5
12	27.6	182	15.2	28.8	186	15.5	25.5	175	14.6
15	18.4	166	11.1	19.1	169	11.3	15.0	150	10.0
20	10.4	144	7.2	10.0	142	7.1	8.0	127	6.3
30	4.7	118	3.9	4.2	113	3.8	3.5	102	3.4

FIGURE 2

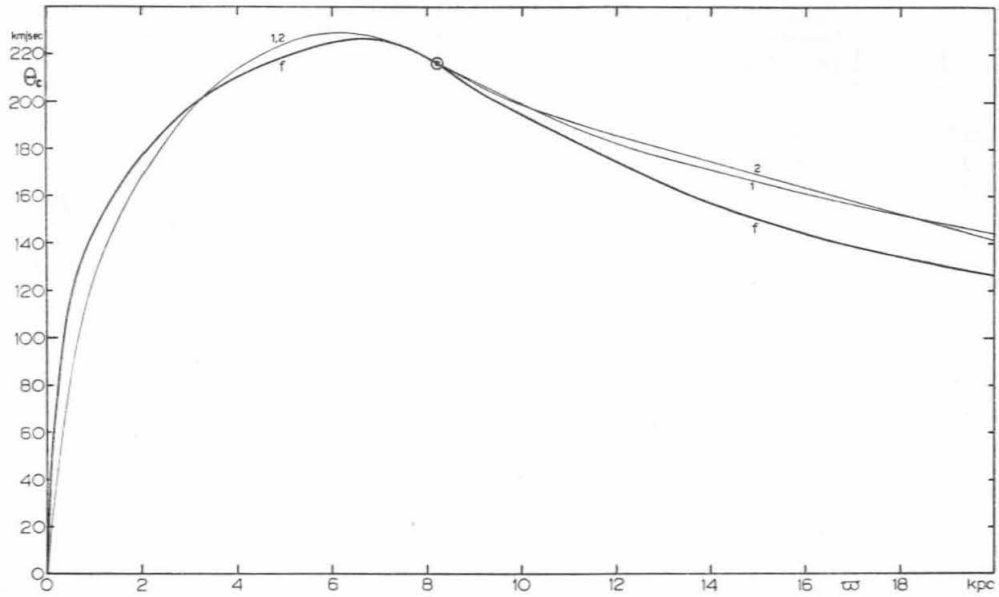

Circular velocities in the first, second and final model, indicated by 1, 2 and *f* respectively.

Accurate values of the potential Φ in the galactic plane are given in Table 10. Beyond distances of 40 kpc the potential is

$$\Phi = \frac{301200}{\varpi},$$

in km²/sec², if ϖ is expressed in kpc.

The potential $\Phi_\odot$ at the sun's position is found to be

$$\Phi_\odot = 41020 \text{ km}^2/\text{sec}^2.$$

This corresponds to a velocity of escape of 286.5 km/sec. The circular velocity near the sun is 216.5 km/sec, so that a star with a residual velocity of 70 km/sec in the direction of $l = 57°$, $b = 0°$ would escape from the system. This result gives some support to the hypothesis advanced long ago by J. H. OORT [1]), that the limiting velocity of about 65 km/sec observed in the general direction of the rotation of the Galactic System represents the difference between the velocity of escape and the circular velocity. It should be noted that the potential is not extremely well determined. It depends somewhat on the exact form of the rotation curve of neutral hydrogen in the innermost parts of the system, which is still poorly determined. Further, the potential and the mass would increase somewhat if we would replace the outer part of the fourth spheroid by a more extended spheroidal shell.

The mean value of K_z at $\varpi = 8.2$ kpc in an interval of z from 2 to 10 kpc is 1900, or 6.2×10^{-9} cm/sec². This is about 30% lower than the value found by OORT and VAN WOERKOM (cf. section 5d.) The density gradient of RR Lyrae variables, which they used, was taken from an investigation by SHAPLEY of southern fields with $-b > 40°$. It may be seen from Figure 5 that K_z at, say, $z = 4$ kpc varies with a factor of 4 over the region with latitude greater than 40°. From this point of view, the agreement between the value of K_z from the observations and the value in our model, both in the interval of z from 2 to 10 kpc, may be considered to be satisfactory.

A very recent determination of K_z by HILL [2]) from

TABLE 10

Potential Φ in units of 100 km²/sec², in the galactic plane.

ϖ (kpc)	Φ ($\times$ 100 km²/sec²)	ϖ (kpc)	Φ ($\times$ 100 km²/sec²)
0.0	1436.5	9	369.0
0.5	1314.5	10	327.1
1.0	1197.5	11	293.0
1.5	1102.5	12	265.1
2.0	1019.8	13	242.2
2.5	946.0	14	223.2
3.0	878.3	15	207.1
3.5	816.2	16	193.2
4.0	758.9	17	181.1
4.5	705.7	18	170.5
5.0	656.2	19	161.1
5.5	610.0	20	152.7
6.0	566.7	22	138.3
6.5	526.0	24	126.5
7.0	488.1	26	116.5
7.5	453.4	28	108.1
8.0	421.9	30	100.7
8.2	410.2	35	86.1
		40	75.3

[1]) J. H. OORT, *B.A.N.* **4**, 269, 1928; No. 159.

[2]) E. R. HILL, to be published in *B.A.N.*

TABLE 7

Potential Φ in units of 100 km^2/sec^2.

ϖ (kpc)	0	2.05	3.075	4.10	5.125	6.15	7.175	8.20	9.225	10.25	11.275	12.30	14.35	16.40
z (kpc)														
0	1436	1012	869	748	644	554	475	410	358	318	285	258	217	188
0.1	1373	1003	864	745	642	553	475	410	358	318	285	258	217	188
0.2	1313	991	856	740	639	551	474	409	358	318	285	258	217	188
0.4	1208	959	834	725	630	544	470	407	357	317	285	258	217	188
0.7	1085	904	797	700	611	531	462	402	353	315	284	257	217	188
1	989	851	762	675	592	518	453	396	349	312	282	257	217	188
1.5	866	775	705	630	560	495	438	386	343	308	280	256	216	188
2	771	706	650	591	531	473	422	376	336	304	278	254	215	187
3	636	605	562	522	478	433	391	354	320	292	269	247	211	185
4	539	520	491	460	428	395	362	332	304	280	259	239	207	183
5	466	458	438	414	388	361	335	312	290	268	247	229	200	180
7	367	362	355	339	323	306	289	273	258	243	228	212	189	171
10	275	270	266	260	254	247	238	228	218	208	198	188	170	156
14	204	203	201	199	195	190	185	180	175	170	165	159		
18	160	160	159	158	156	154	152	150	148	145				

TABLE 8

Force K_{ϖ} in units of 100 km^2/sec^2. kpc $= 0.324 \times 10^{-9}$ cm/sec^2.

ϖ (kpc)		2.05	3.075	4.10	5.125	6.15	7.175	8.20	9.225	10.25	11.275	12.30	14.35	16.40
z (kpc)														
0		155	128	109	94	82	70	57	44	36	29	23.8	16.5	12.3
0.1		153	128	109	94	82	70	57	44	36	29	23.8	16.5	12.3
0.2		146	124	107	93	82	70	57	44	36	29	23.8	16.5	12.3
0.4		130	115	102	90	79	67	55	43	35	29	23.6	16.4	12.2
0.7		112	102	91	82	74	63	52	41	34	28	23.3	16.2	12.1
1		93	89	83	76	69	60	50	40	33	27	22.9	16.0	12.0
1.5		69	72	70	65	59	52	45	38	31	26	22.0	15.6	11.8
2		50	58	61	57	53	47	41	35	30	25	21.2	15.1	11.5
3		32	39	43	44	42	38	34	30	26	23	19.6	14.4	11.1
4		21.4	27	32	34	33	31	28	25	22.5	20.0	17.8	13.3	10.6
5		15.1	19.6	23	25	25	24	23	21.4	19.5	17.7	15.9	12.7	10.0
7		8.0	10.9	13.6	15.4	16.2	16.4	16.2	15.6	14.8	13.7	12.5	10.3	8.8
10		3.9	5.6	7.0	8.1	9.0	9.4	9.5	9.5	9.3	9.0	8.6	7.8	7.0
14		1.8	2.5	3.1	3.7	4.2	4.6	4.9	5.1	5.2	5.2	5.2	5.0	4.6
18		0.9	1.2	1.7	2.0	2.3	2.6	2.8	3.0	3.1				

TABLE 9

Force K_z in units of 100 km^2/sec^2. kpc $= 0.324 \times 10^{-9}$ cm/sec^2.

ϖ (kpc)	0	2.05	3.075	4.10	5.125	6.15	7.175	8.20	9.225	10.25	11.275	12.30	14.35	16.40
z (kpc)														
0.1	625	92	50	34	25	15	9.4	5.6	3.3	2.0	1.0	0.6	0.2	0.1
0.2	575	142	95	62	42	28	16.0	8.9	5.7	3.6	2.0	1.1	0.3	0.1
0.4	474	174	115	79	58	41	25	13.8	8.6	5.4	3.2	1.9	0.6	0.2
0.7	358	183	130	88	64	44	28	17.3	10.9	6.8	4.3	2.8	1.1	0.4
1	286	172	130	90	66	45	30	19.1	12.3	7.8	5.3	3.6	1.6	0.6
1.5	217	149	116	85	65	45	31	20.8	13.9	9.1	6.4	4.6	2.2	1.0
2	169	129	104	80	59	44	31	21.8	15.0	10.2	7.4	5.4	2.7	1.3
3	113	98	81	65	51	40	30	22.7	16.3	11.8	8.9	6.8	3.8	2.0
4	84	74	63	53	44	36	29	22.1	17.0	12.8	10.0	7.7	4.9	2.6
5	64	56	49	43	37	32	26	20.6	16.4	13.0	10.6	8.5	5.6	3.2
7	41	38	35	32	28	24	20.6	17.2	14.5	12.4	10.6	9.1	6.7	4.4
10	24	24	23	21	18.9	17.0	15.2	13.4	11.8	10.3	9.0	7.9	6.2	5.1
14	13.4	13.1	12.6	12.0	11.3	10.6	9.9	9.2	8.4	7.7	7.0	6.3	5.2	4.4
18	8.6	8.1	8.0	7.8	7.5	7.2	7.0	6.7	6.4	6.0	5.7	5.4		

FIGURE 3

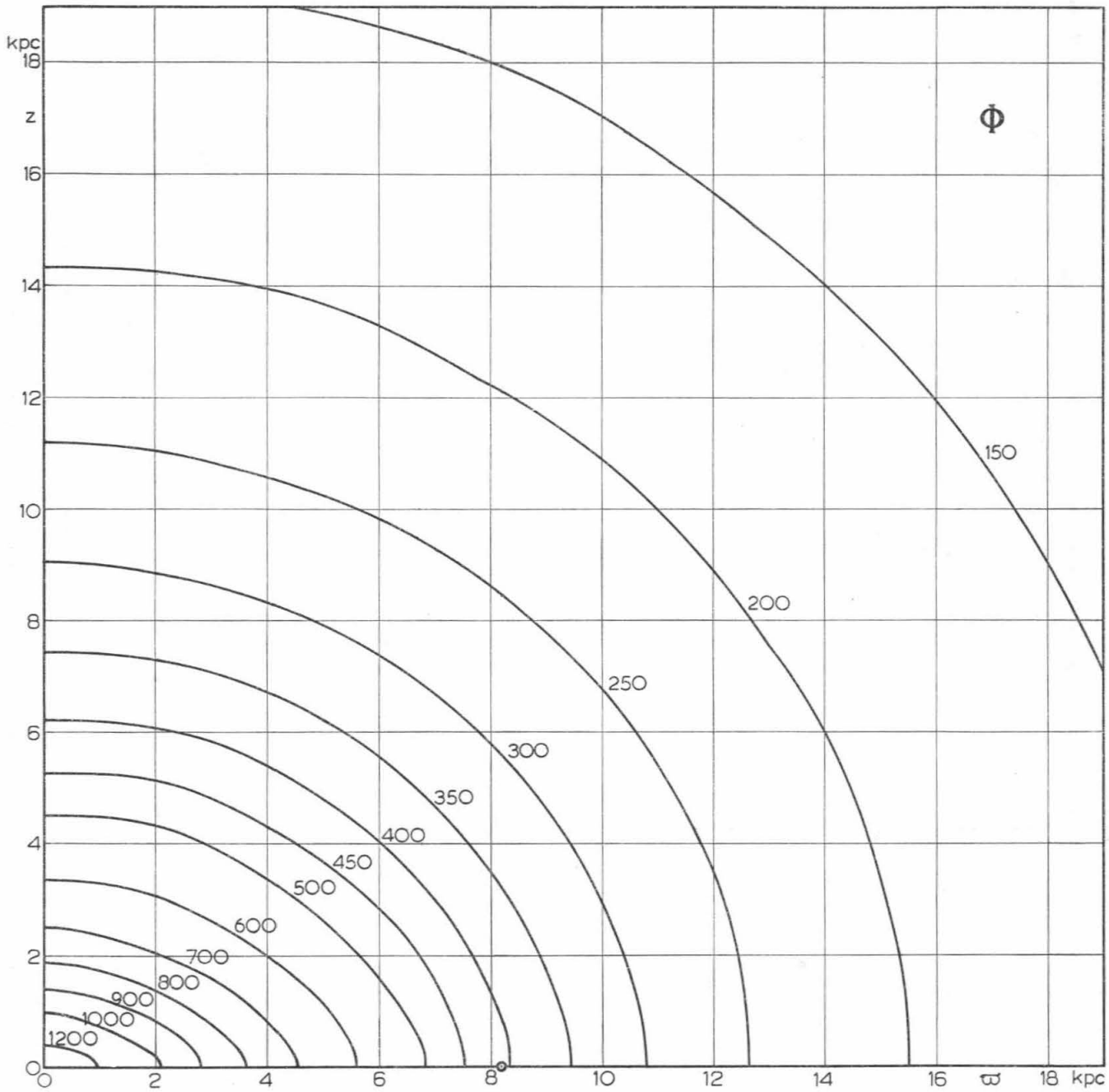

Potential Φ in units of 100 km²/sec², in the (ϖ,z)-plane.

FIGURE 4

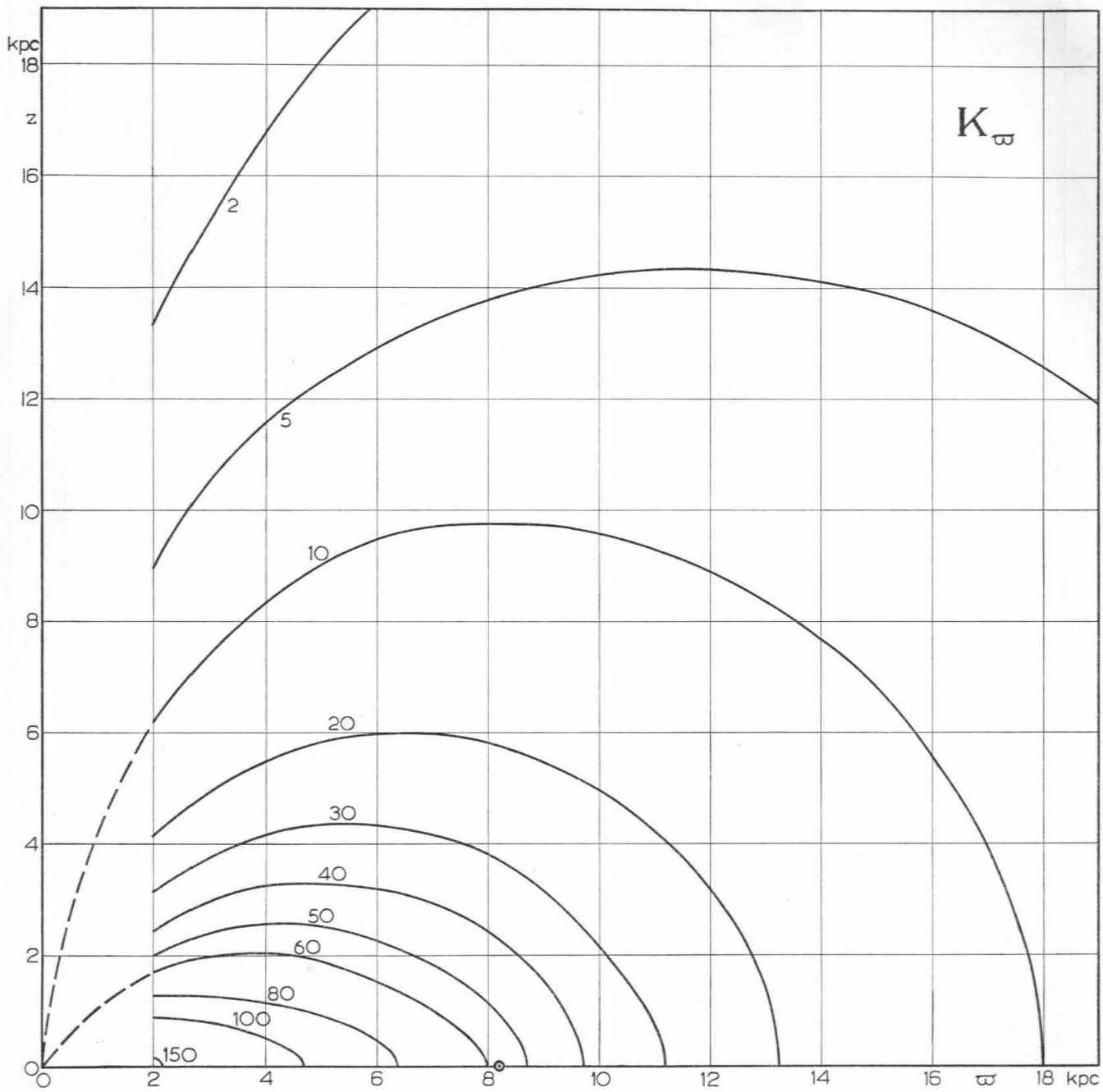

Force K_{ϖ} in units of 100 km^2/sec^2. kpc = 0.324 × 10^{-9} cm/sec^2, in the (ϖ,z)-plane.

FIGURE 5

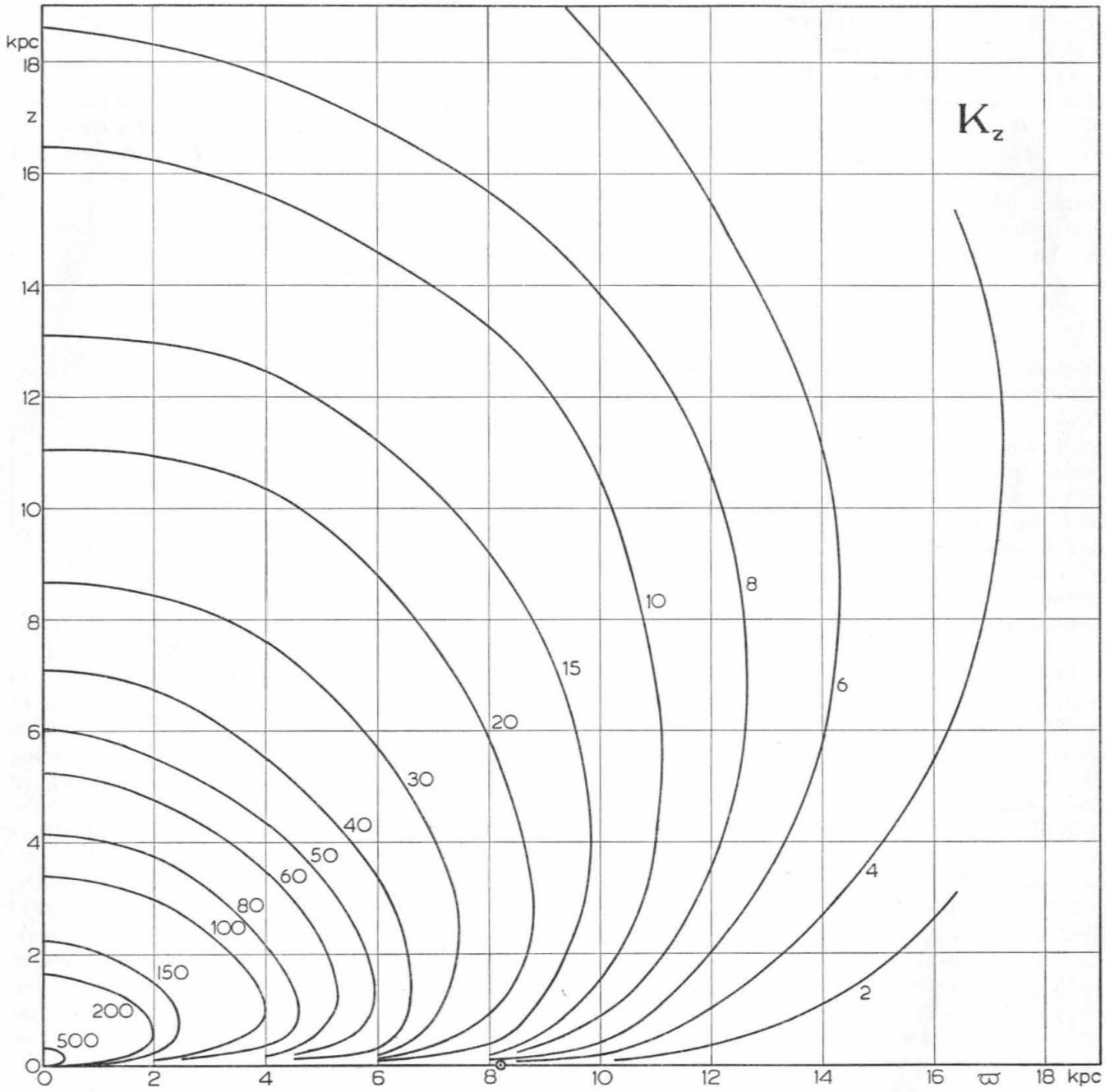

Force K_z in units of 100 km^2/sec.^{2} kpc = 0.324 × 10^{-9} cm/sec^2, in the (ϖ,z) plane.

density and velocity distribution of K stars points to lower values of K_z at high altitude. He finds $K_z = 4.4 \times 10^{-9}$ cm/sec^2 or 14 km^2/sec^2.kpc at $z = 1$ kpc, while the model gives 19 km^2/sec^2.kpc.

The mean turbulent velocity in the galactic plane of neutral hydrogen [1]) at $\varpi = 1.5$ kpc is of the order of 50 km/sec. At this position our model yields $\sigma_Z = 25$ km/sec in the first spheroid. If the velocity dispersions in the plane and perpendicular to the plane would be equal, the mass distribution near the centre should be still more concentrated to the galactic plane, which does not seem probable.

13. *The distribution of globular clusters.*

The distribution of globular clusters was studied originally with the purpose of determining the form of surfaces of equal potential in the Galactic System. It was hoped that this would yield an indication of the axial ratio of the mass spheroids. However, the form of the equipotential surfaces varies only very slightly with the form of the mass distribution, as may be seen by comparing Figures 1 and 3. The space distribution of globular clusters, which was obtained, showed some interesting features. It will be described in the present section; a short discussion of the velocity distribution will be given in the next section.

The distribution of globular clusters has previously been studied by DE KORT [2]) and OORT [3]). DE KORT studied the surface distribution on the sky, excluding the central parts and a belt along the galactic equator. He found a small amount of flattening in the distribution. OORT essentially studied the distribution in a strip of low galactic latitude, to reduce the variation in absorption, and compared it with the distribution to be expected from different mass models.

In the present section we shall try to determine the distribution in space directly from positions and distances. Again the absorption is a major difficulty. In the present investigation it has been tried to overcome this difficulty by considering only those clusters which are situated in a region where all clusters may be supposed to have been discovered. Such a region may be obtained as follows. The absorption suffered by the light from a globular cluster is supposed to be due mainly to dust particles concentrated in a narrow layer in the galactic plane. We take HUBBLE's value of $0^m.25$ for the absorption towards the galactic pole. Then

$$m = M - 5 + 5 \log r + 0.25 \operatorname{cosec} b. \quad (13,1)$$

The absolute magnitude of the faintest globular clusters is about -5^M. If we assume that all globular clusters brighter than $11^m.5$ have been discovered, the absolutely faintest cluster is still found, if

$$11.5 > -10 + 5 \log r + 0.25 \operatorname{cosec} b,$$

or, if the distance r is expressed in kpc,

$$\log r + 0.05 \operatorname{cosec} b < 1.3. \quad (13,2)$$

Therefore we may expect that all globular clusters in the volume defined by (13,2) are known. Figure 6

FIGURE 6

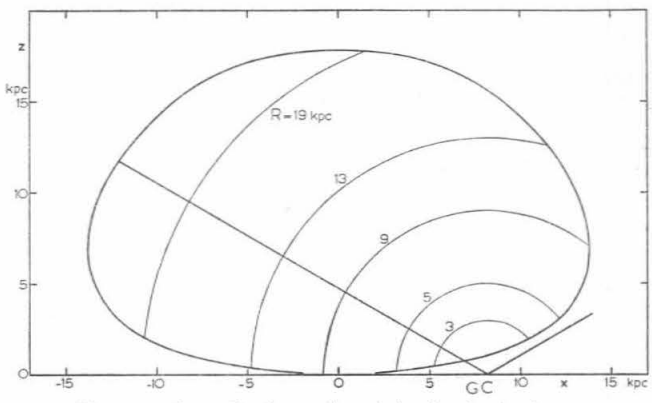

Cross section of volume (13,2) in the (x,z)-plane. The galactic centre is indicated by GC.

shows a cross section through this volume in the (x,z)-plane. The galactic centre is indicated at $x = 8.2$ kpc. Further, cross sections are drawn with different spheres around the galactic centre. Table 11 gives data for 54 clusters with known distances which satisfy (13,2). C_s is the concentration class according to SHAPLEY [4]), r the distance from the sun taken from an investigation by LOHMANN [5]), x, y and z are the distance components reckoned from the sun in directions $l = 327°$, $b = 0°$; $l = 57°$, $b = 0°$ and $b = 90°$, respectively; R is the distance from the galactic centre. Now the obvious procedure is to count the number of clusters in spherical shells concentric with the galactic centre. The determination of the volume cut out of volume (13,2) by various spherical shells was found by numerical integration. Each shell was further divided into a polar and an equatorial part by a cone centred on the galactic centre. The surface of the cone has an inclination of $27\frac{1}{2}°$ to the galactic plane. Its cross section with the (x,z)-plane is indicated in Figure 6. This cone divides the globular clusters in two equal groups. Table 12 gives the numbers, volumes and resulting space densities.

Although the numbers are small, a distinct flattening may be noted. However, we first investigate the relatively large number of clusters in the equatorial part of the shell 5 — 9 kpc. The table shows a nearly constant density between 3 and 9 kpc, but a forty

[1]) K. K. KWEE, C. A. MULLER, and G. WESTERHOUT, *B.A.N.* **12**, 211, 1954; No. 458.
[2]) J. DE KORT, *B.A.N.* **9**, 189, 1941; No. 338.
[3]) J. H. OORT, *B.A.N.* **9**, 193, 1941; No. 338.
[4]) H. SHAPLEY, "Star Clusters".
[5]) W. LOHMANN, *Zs. f. Ap.* **30**, 234, 1952.

TABLE 11

Data for globular clusters inside volume (13,2).

NGC	C_s	r kpc	x kpc	y kpc	z kpc	R kpc	NGC	C_s	r kpc	x kpc	y kpc	z kpc	R kpc
104	III	5.2	+ 2.1	− 3.0	− 3.7	7.7	6287	VII	8.7	+ 8.5	+ 0.2	+ 1.5	1.5
288	X	13.2	− 0.5	− 0.1	−13.2	15.8	6333	VIII	6.3	+ 6.1	+ 0.6	+ 1.1	2.4
362	III	10.5	+ 3.7	− 6.1	− 7.6	10.8	6341	IV	9.6	+ 2.8	+ 7.4	+ 5.5	10.7
1851	II	13.2	− 4.6	− 9.8	− 7.5	17.8	6352	XI	4.6	+ 4.3	− 1.4	− 0.6	4.2
2808	I	6.9	+ 1.3	− 6.7	− 1.3	9.7	6356	II	10.0	+ 9.7	+ 1.2	+ 1.6	2.5
3201	X	2.9	+ 0.3	− 2.8	+ 0.4	8.4	6362	X	5.8	+ 4.6	− 3.1	− 1.8	5.1
4372	XII	3.2	+ 1.7	− 2.7	− 0.6	7.1	6366	XI	2.4	+ 2.2	+ 0.8	+ 0.6	6.1
4590	X	11.0	+ 4.7	− 7.6	+ 6.5	10.6	6388	III	8.3	+ 8.0	− 2.0	− 1.2	2.3
4833	VIII	4.6	+ 2.5	− 3.8	− 0.6	6.9	6397	IX	2.4	+ 2.2	− 0.9	− 0.5	6.1
5053	XI	15.1	+ 3.1	− 0.9	+14.8	15.7	6402	VIII	6.3	+ 5.7	+ 2.3	+ 1.5	3.7
5139	VIII	4.6	+ 2.8	− 3.4	+ 1.2	6.5	6496	XII	6.0	+ 5.8	− 1.2	− 1.1	2.8
5272	VI	9.6	+ 1.6	+ 1.3	+ 9.4	11.6	6539	X	1.6	+ 1.5	+ 0.6	+ 0.1	6.7
5286	V	8.7	+ 5.8	− 6.2	+ 1.5	6.9	6541	III	4.2	+ 4.1	− 0.7	− 0.8	4.2
5466	XII	14.5	+ 3.2	+ 2.9	+13.8	15.0	6553	XI	1.3	+ 1.3	+ 0.1	− 0.1	6.9
5897	XI	12.0	+10.1	− 2.7	+ 5.8	6.8	6569	VIII	7.2	+ 7.1	+ 0.1	− 0.9	1.4
5904	V	9.1	+ 6.2	+ 0.5	+ 6.6	6.9	6584	VIII	12.6	+11.4	− 3.6	− 3.7	6.1
5927	VIII	3.2	+ 2.6	− 1.7	+ 0.2	5.9	6626	IV	4.0	+ 3.9	+ 0.6	− 0.5	4.4
6093	II	10.5	+ 9.9	− 1.1	+ 3.2	3.8	6637	V	6.0	+ 5.9	+ 0.2	− 1.2	2.6
6101	X	9.1	+ 6.4	− 5.9	− 2.5	6.7	6656	VII	3.0	+ 2.8	+ 0.5	− 0.5	5.4
6121	IX	2.2	+ 2.1	− 0.3	+ 0.6	6.1	6715	III	10.5	+10.1	+ 1.0	− 2.7	3.4
6144	XI	10.0	+ 9.5	− 1.3	+ 2.6	3.4	6723	VII	10.5	+10.0	+ 0.2	− 3.5	3.9
6171	X	2.6	+ 2.4	+ 0.2	+ 1.0	5.9	6752	VI	5.0	+ 4.0	− 1.8	− 2.3	5.1
6205	V	6.6	+ 2.6	+ 4.4	+ 4.2	8.3	6760	IX	2.1	+ 1.7	+ 1.2	− 0.2	6.6
6218	IX	5.8	+ 5.0	+ 1.5	+ 2.4	4.3	6809	XI	6.9	+ 6.2	+ 0.9	− 2.9	3.6
6254	VII	5.5	+ 4.9	+ 1.4	+ 2.1	4.2	7078	IV	12.0	+ 4.3	+ 9.7	− 5.6	11.9
6266	IV	6.3	+ 6.2	− 0.5	+ 0.8	2.2	7089	II	14.5	+ 6.9	+ 9.6	− 8.6	13.0
6273	VIII	5.8	+ 5.7	− 0.2	+ 0.9	2.7	7099	V	12.0	+ 7.1	+ 3.8	− 9.0	9.8

TABLE 12

Space densities of globular clusters.

	Equatorial part			Polar part		
R kpc	number	volume kpc^3	density kpc^{-3}	number	volume kpc^3	density kpc^{-3}
1 − 3	4	2.10	1.90	5	51.2	0.098
3 − 5	4	16.6	0.24	7	253	0.028
5 − 9	17	130	0.13	5	1552	0.0032
9 − 13	1	333	0.003	6	3070	0.0020
13 − 19	1	854	0.001	4	5490	0.0007

TABLE 13

Space densities of globular clusters of concentration classes I-VIII.

	Equatorial part		Polar part	
R kpc	number	density kpc^{-3}	number	density kpc^{-3}
1 − 3	3	1.43	5	0.098
3 − 5	3	0.18	4	0.016
5 − 9	5	0.039	4	0.0026
9 − 13	1	0.003	5	0.0016
13 − 19	1	0.001	1	0.0002

times smaller density in the shell 9 − 13 kpc. Inspection of the data shows that the shell 5 − 9 kpc contains a relatively large number of clusters with concentration classes IX-XII, which are very loose clusters. This suggests that for clusters of concentration classes IX-XII there still exists a very large selection effect, primarily with distance. Indeed, 8 of the 11 clusters of class IX-XII in the shell 5 − 9 kpc have distances of less than 3 kpc from the sun. The three remaining clusters are at distances of 9, 10 and 12 kpc, which shows that not all loose clusters are nearby. The safest procedure seems to exclude all globular clusters with concentration classes IX-XII.

Table 13 gives the numbers and densities for classes I-VIII only. The run of the densities in the equatorial part is now found to be much smoother. It appears possible to represent the equatorial and the polar densities by the following analytical formulae:

$$\rho_e = 100 \times 10^{-1.34\sqrt{R}}, \qquad (13,3)$$

$$\rho_p = \quad 2 \times 10^{-1.00\sqrt{R}}. \qquad (13,4)$$

The deviations are not larger than expected from statistical fluctuations. The flattening of the system of globular clusters may be obtained by putting $\rho = \rho_p$ and comparing the values of R_e and R_p.

Table 14 gives the ratio $\frac{R_p}{R_e}$, which is roughly the axial ratio of the surfaces of constant space density, as a function of ϖ, which is practically R_e. There appears to be a systematic decrease of the flattening of the system outwards. This decrease of flattening is certainly real, as it is also obtained by comparing the densities in the equatorial and polar shells at once, without using the smooth density runs of (13,3) and (13,4).

TABLE 14

Axial ratio of surfaces of constant space density in the system of globular clusters.

ϖ kpc	R_p/R_e
4	0.24
9	0.60
16	0.84

From (13,3) and (13,4) the total number of globular clusters of concentration classes I-VIII may be estimated to be about 160. The total number of observed clusters of these classes is 62.

14. *The velocity distribution of globular clusters.*

Many authors have, in the course of time, tried to determine the relative velocity of the sun with respect to the system of globular clusters. We shall try to obtain some information about the differential rotation and the distribution of peculiar velocities in the cluster system. Since the publication of MAYALL's beautiful set of radial velocities, several authors have studied the velocity distribution of globular clusters. MAYALL [1]) himself states that "no satisfactory interpretation of the individual peculiar velocities in terms of a differential or general rotation has been found". Assuming a circular velocity near the sun of 275 km/sec, PEREK [2]) found a retrograde motion of the system of − 160 km/sec at 1 kpc, − 100 km/sec at 6 kpc and of − 130 km/sec at 15 kpc from the centre. He used analytical formulae to represent the rotational velocity of the clusters as a function of ϖ and z, which may be a dangerous procedure when so little is known about the rotation. VON HOERNER [3]) tried to distinguish between the cases of straight-line orbits through the centre and of circular orbits. He conclud-

[1]) N. U. MAYALL, *Ap. J.* **104**, 290, 1946.
[2]) L. PEREK, *Ann. d'Ap.* **11**, 185, 1948.
[3]) S. VON HOERNER, *Zs. f. Ap.* **35**, 255, 1955.

TABLE 15

Radial velocities and rotational components of globular clusters.

NGC	C_s	Rad. vel. km/sec	V_r km/sec	cos φ	$\frac{V_r}{\cos\varphi}$ km/sec	NGC	C_s	Rad. vel. km/sec	V_r km/sec	cos φ	$\frac{V_r}{\cos\varphi}$ km/sec
1851	II	+ 291	+ 112	−0.38	− 296	6341	VIII	+ 224	+ 258	+0.36	+ 726
1904	V	+ 231	+ 72	− .25	− 288	6356	II	+ 31	+ 70	+ .52	+ 135
2298	VI	+ 64	− 147	− .28	+ 520	6402	VIII	− 131	− 36	+ .88	− 41
2419	VII	+ 14	+ 5	− .00	−	6440	V	− 133	− 87	+ .22	− 394
4147	IX	+ 191	+ 154	− .16	− 993	6441	III	− 70	− 65	− .09	−
4590	X	− 116	− 267	− .68	+ 396	6544		− 12	+ 22	+ .12	+ 182
5024	V	− 112	− 120	− .12	+1000	6624	VI	+ 69	+ 90	+ .11	+ 788
5272	VI	− 150	− 114	+ .17	− 626	6626	IV	+ 1	+ 44	+ .29	+ 154
5634	IV	− 63	− 95	− .27	+ 346	6637	V	+ 95	+ 111	+ .12	+ 932
5694		− 187	− 315	− .13	+2365	6638	VI	− 14	+ 28	+ .18	+ 151
5824	I	− 58	− 133	− .16	+ 805	6652	VI:	− 124	− 109	+ .03	−
5904	V	+ 45	+ 70	+ .21	+ 327	6656	VII	− 148	− 100	+ .25	− 396
5986	VII	+ 2	− 72	− .41	+ 175	6681	V	+ 198	+ 218	+ .04	−
6093	II	+ 18	+ 3	− .48	− 6	6712	IX:	− 131	− 19	+ .99	− 19
6171	X	− 147	− 117	+ .11	−1073	6715	III	+ 107	+ 138	+ .37	+ 371
6205	V	− 228	− 65	+ .77	− 85	6723	VII	− 3	+ 9	+ .09	−
6218	IX	+ 36	+ 108	+ .61	+ 178	6779	X	− 154	+ 54	+ .58	+ 93
6229	VII:	− 150	+ 26	+ .32	+ 80	6838		− 80	+ 118	+ .97	+ 121
6254	VII	+ 73	+ 144	+ .58	+ 248	6864	I	− 222	− 149	+ .20	− 726
6266	IV	− 81	− 89	− .31	+ 287	6934	VIII	− 360	− 183	+ .49	− 375
6273	VIII	+ 102	+ 106	− .11	− 939	6981	IX	− 255	− 140	+ .38	− 364
6284	IX:	+ 22	+ 29	− .02	−	7006	I	− 348	− 150	+ .17	− 866
6293	IV	− 73	− 70	− .06	−	7078	IV	− 114	+ 74	+ .63	+ 117
6304	VI	− 98	− 102	− .15	+ 698	7089	II	− 3	+ 151	+ .56	+ 271
6333	IV	− 118	+ 68	+ .68	+ 99	7099	V	− 164	− 91	+ .65	− 140

ed, mainly from a scatter diagram of the normalized radial velocity u_0 (being the ratio of radial velocity and circular velocity) against the angle θ between the directions to the centre and the sun as seen from the cluster, that most clusters would have straight or highly eccentric orbits. Part of the decrease of scatter in u_0 with increasing values of θ may be due however to the Π dispersion being greater than both the Θ and Z dispersions. On the other hand we would expect many elongated orbits a priori, because the dispersion of the space velocities of globular clusters is of the same order as the circular velocities in the Galactic System. PARENAGO's work on the velocity distribution of globular clusters will be discussed later in this section.

In the present investigation it is assumed that the system of globular clusters is in well-mixed condition. In that case we may expect in each element of volume zero average Π and Z velocities. The average Θ velocity will be $\overline{\Theta}$. If the angle between the direction of $\overline{\Theta}$ and the direction to the sun as seen from the cluster is φ, the rotational velocity gives a radial velocity component

$$V_r = \overline{\Theta} \cos \varphi. \qquad (14,1)$$

The angle φ is easily calculated from

$$\cos \varphi = -\frac{8.2}{r} \frac{Y}{\sqrt{X^2 + Y^2}}, \qquad (14,2)$$

where r is the distance of the cluster from the sun; X, Y are its galactic rectangular co-ordinates measured from the centre. The large peculiar velocities of globular clusters will make (14,1) useless for individual clusters. It should be used to determine the rotational velocity statistically.

The third column of Table 15 gives MAYALL's radial velocities. These were corrected for the effect of the sun's velocity with respect to the circular velocity, with the aid of LINK's [1]) tables, which are based on a velocity of 20 km/sec towards $\alpha = 18^h$, $\delta = +30°$. The resulting radial velocities have been reduced to velocities V_r with respect to the galactic centre by subtracting the component due to the circular velocity of 216 km/sec near the sun. The tabulated values of cos φ show that only 13 clusters have a value of cos φ greater than 0.50. This is a most unfavourable circumstance because the smaller the value of cos φ, the larger is the effect of the peculiar velocities on $\overline{\Theta}$. The mean rotational velocity was determined in four ranges of $\varpi = \sqrt{X^2 + Y^2}$, as shown in Table 16. All clusters with $|\cos \varphi| > 0.1$ were included in the solution, a weight proportional to $\cos^2 \varphi$ being assigned to each cluster. The errors indicated are mean errors based on a value of $\pm$ 120 km/sec for the dispersion in V_r. The table clearly shows that no detailed information can be obtained about the rotational velocity as a function of ϖ.

TABLE 16

Rotational velocities $\overline{\Theta}$ of the system of globular clusters and their mean errors.

ϖ kpc	$\overline{\varpi}$ kpc	$\overline{\Theta}$ km/sec
0 – 4	2.8	+ 76 ± 61 (m.e.)
4 – 8	6.3	+ 39 ± 84
8 – 13	10.5	+111 ± 77
13 – 26	20	+ 59 ±175

A positive, or direct, rotation of the order of 80 km/sec is indicated.

The dispersion of the Π velocities was obtained from 37 clusters for which $|\cos \varphi| > 0.5$. We get $\sigma_\Pi = 124$ km/sec with a mean error of 15 km/sec. Extensive trials have been made with a few assumed runs of the rotational velocity with ϖ, to get an estimate of the variation of σ_Θ with ϖ. No significant results were obtained. These negative results fully confirm MAYALL's statement quoted before. Therefore it is somewhat surprising that PARENAGO [2]) from the same radial velocities obtained a curve of rotational velocities which seems to be well established up to 8 kpc from the centre. However, the mean errors appear to have been underestimated. A direct determination of the mean errors of the rotational velocities from the residuals (rotational velocity observed minus average rotational velocity) with the standard formula,

$$\text{m.e.} = \frac{\Sigma p (O - C)^2}{(n - 1) \Sigma p},$$

yields values which are about 2 times the mean errors indicated in PARENAGO's Table 4.

15. *Forces due to a spiral arm.*

In all calculations of potentials in the Galactic System at large, one is forced to assume axial symmetry of the system. However, the potential will deviate systematically in regions of about 1 kpc width in the ϖ direction, due to the gravitational effect of spiral arms, in which population I objects tend to concentrate. In the present section we shall investigate the deviations to be expected as a consequence of this phenomenon.

The surface density σ, as projected on the galactic plane, of a non-homogeneous spheroid is

$$\sigma = 2 \int_0^{\sqrt{(1-e^2)(a_r^2 - \varpi^2)}} \varrho \, dz. \qquad (15,1)$$

[1]) F. LINK, *Mem. and Obs. Czechosl. Astr. Soc.* No. 9, 1948.

[2]) P. P. PARENAGO, *A.J. U.S.S.R.* **24**, 167, 1947.

If the space density ρ is given by

$$\rho = \frac{\sigma}{\pi\sqrt{(1-e^2)(a_r^2-a^2)}}, \qquad (15,2)$$

the surface density σ in the non-homogeneous spheroid is found to be constant. Then, by (2,21)

$$K_\varpi = 4e^{-3}\varpi\sigma\int_0^\gamma \frac{\sin^2\beta}{\sqrt{a_r^2-a^2}}\,d\beta, \qquad (15,3)$$

in which β is obtained from (2,10) and γ from (2,20) for external points; for internal points $\gamma = \arcsin e$. If we now take $e = 1$, we get for a disc of constant surface density σ

$$K_\varpi = 4\varpi\sigma\int_0^\gamma \frac{\sin^2\beta}{\sqrt{a_r^2-a^2}}\,d\beta, \qquad (15,4)$$

with $\varpi^2\sin^2\beta + z^2\operatorname{tg}^2\beta = a^2$

and $\varpi^2\sin^2\gamma + z^2\operatorname{tg}^2\gamma = a_r^2$ for external points, while for internal points $\gamma = \frac{\pi}{2}$.

For an internal point in the galactic plane,

$$K_\varpi = \frac{4\varpi\sigma}{a_r}\int_0^{\pi/2} \frac{\sin^2\beta}{\sqrt{1-\frac{\varpi^2}{a_r^2}\sin^2\beta}}\,d\beta,$$

$$= \frac{4\varpi\sigma}{a_r}\mathbf{D}(k), \quad \text{where } k = \frac{\varpi}{a_r}. \qquad (15,5)$$

$\mathbf{D}(k)$ may be expressed in Legendre's complete elliptic integrals of the first and second kind [1]):

$$\mathbf{D}(k) = \frac{\mathbf{K}-\mathbf{E}}{k^2}.$$

For an external point in the galactic plane,

$$K_\varpi = \frac{4\varpi\sigma}{a_r}\int_0^{\arcsin\frac{a_r}{\varpi}} \frac{\sin^2\beta}{\sqrt{1-\frac{\varpi^2}{a^2}\sin^2\beta}}\,d\beta,$$

which may be transformed to complete elliptic integrals by substituting $\alpha = \arcsin\left(\frac{\varpi}{a_r}\sin\beta\right)$.

In the plane we get for internal and external points, respectively,

$$K_\varpi = 4\sigma k\mathbf{D}(k) = 4\frac{\sigma}{k}(\mathbf{K}-\mathbf{E}), \quad k = \frac{\varpi}{a_r} < 1, \qquad (15,6)$$

$$K_\varpi = 4\sigma k^2\mathbf{D}(k) = 4\sigma(\mathbf{K}-\mathbf{E}), \quad k = \frac{\varpi}{a_r} > 1. \qquad (15,7)$$

[1]) JAHNKE und EMDE, "Funktionentafeln".

The force due to a flat ring is computed as the difference of the forces due to two discs with equal σ and different a_r. A major objection to a circular flat ring is that the forces at the boundaries are infinite. Therefore we shall represent a spiral arm by a three-dimensional ring composed of an infinite number of flat rings with surface density $d\sigma$. We then need the force K_ϖ at a point not in the plane of a flat disc. This is

$$K_\varpi = 4\sigma\varpi\int_0^\gamma \frac{\sin^2\beta\,d\beta}{\sqrt{a_r^2-\varpi^2\sin^2\beta-z^2\operatorname{tg}^2\beta}}.$$

Putting

$$\lambda^2 = \tfrac{1}{2}\left(\frac{a_r^2}{\varpi^2}+1+\frac{z^2}{\varpi^2}\right) - \sqrt{\tfrac{1}{4}\left(\frac{a_r^2}{\varpi^2}+1+\frac{z^2}{\varpi^2}\right)^2-\frac{a_r^2}{\varpi^2}},$$

$$\mu^2 = \tfrac{1}{2}\left(\frac{a_r^2}{\varpi^2}+1+\frac{z^2}{\varpi^2}\right) + \sqrt{\tfrac{1}{4}\left(\frac{a_r^2}{\varpi^2}+1+\frac{z^2}{\varpi^2}\right)^2-\frac{a_r^2}{\varpi^2}},$$

and $k = \frac{\lambda}{\mu}$,

we get

$$K_\varpi = 4\sigma k\lambda\mathbf{D}(k) = 4\sigma\mu(\mathbf{K}-\mathbf{E}). \qquad (15,8)$$

This is the central force at a point (ϖ,z) due the disc. Again the force due to a ring is obtained by subtracting the forces due to two discs. The total force due to a three-dimensional ring may be obtained by integrating the forces due to the flat rings of which it is composed,

$$K_\varpi = \int f(z)\,d\sigma = \int f(z)\,\rho\,dz, \qquad (15,9)$$

where $f(z)\,d\sigma$ is the force due to a flat ring with surface density $d\sigma$, from (15,8).

As an example we calculate the force in the galactic plane due to the Orion arm, which is the spiral arm containing the sun. We take the following rough model of the Orion arm. A ring with elliptical cross section extending between $\varpi = 8.3$ and 8.96 kpc and $z = -0.11$ and $+0.11$ kpc is filled with material of a density of 100 units, i.e. 1.58×10^{-24} gr/cm^3 or 0.94 H atoms per cm^3. Calculations of $f(z)$ were carried out for flat rings at $z = 0.01$, 0.02, 0.05, 0.08 and 0.10 kpc for 12 values of ϖ. The resulting $f(z)$ were integrated over z. The forces ΔK_ϖ thus obtained are given in Table 17 and Figure 7.

Near the sun ΔK_ϖ is -61 while the total value of K_ϖ is $+5720$. The force decreases about 1% under

the influence of the arm, which corresponds to a decrease of the circular velocity of 1 km/sec. At $\varpi = 9$ kpc the central force increases with 2% and the circular velocity with 2 km/sec.

TABLE 17

Forces ΔK_ϖ due to the Orion arm, in units of 1 km²/sec². kpc = 3.24 × 10^{-12} cm/sec².

ϖ kpc	ΔK_ϖ km²/sec². kpc
7.0	− 11
7.5	− 18
8.0	− 36
8.2	− 61
8.4	− 66
8.63	+ 7
8.8	+ 59
9.0	+ 88
9.2	+ 48
9.5	+ 31
10.0	+ 20
10.5	+ 14

FIGURE 7

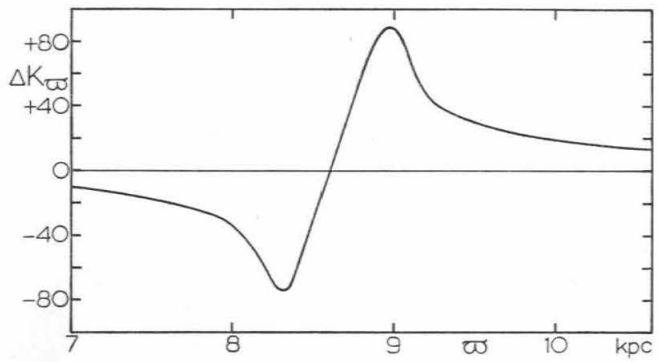

The force ΔK_ϖ due to the Orion arm, in units of 1 km²/sec². kpc = 3.24× 10^{-12} cm/sec².

If we consider a real spiral arm, which is not a ring, the value of ΔK_ϖ will be practically the same. However, a spiral arm will introduce a transversal acceleration K_θ. If the angle between the spiral arm and the radius is $90^\circ - \psi$,

$$K_\theta = \Delta K_\varpi \sin\psi, \qquad (15,10)$$

where ΔK_ϖ is the force due to the spiral only. This is an approximation of course, but it will be sufficient for our purpose, because practically all the acceleration is due to the near part of the spiral. Now let t be the time required to run through one radian of the orbit, so $t = \frac{\varpi}{\Theta}$. After the time t the rotational velocity will have changed by $\Delta\Theta = K_\theta t$. The relative change of the rotational velocity per radian of the orbit is then

$$\frac{\Delta\Theta}{\Theta} = \frac{\Delta K_\varpi}{K_\varpi}\sin\psi. \qquad (15,11)$$

If we take the observed value $\sin\psi = 0.08$, we get near the sun, $\Delta\Theta = +0.18$ km/sec per radian, i.e. per 37×10^6 years, or $\Delta\Theta = +1.2$ km/sec per revolution.

Admittedly, these calculations are rough. We should have taken into account that the sun, due to its peculiar motion, is changing its position with respect to the Orion arm, so that the force due to the arm varies considerably. The results may serve, however, to give an idea of the gravitational influence of a spiral arm. It may well be that population I objects, which are concentrated near the arms and which have only small peculiar motions, are perturbed considerably in their regular epicycle orbits by the gravitation of the spiral arm in which they are situated.

KORT OVERZICHT VAN HET ONDERZOEK

Het volgende overzicht geeft een korte en uiteraard oppervlakkige beschrijving van het onderzoek.

In dit werk wordt een model gegeven van de massaverdeling in het Melkwegstelsel. De massaverdeling in het model is verkregen door vier met materie gevulde rotatie-ellipsoïden van verschillende afmetingen te superponeren. De rotatie-as van ieder der ellipsoïden valt samen met de rotatie-as van het stelsel. In iedere ellipsoïde neemt de dichtheid af van binnen naar buiten. De eerste ellipsoïde geeft ongeveer het dichtheidsverloop van het tussen de sterren zwevende waterstofgas weer. De tweede en derde ellipsoïde tezamen geven het dichtheidsverloop der bekende sterren. In ieder punt van het stelsel kunnen de versnellingen, veroorzaakt door de drie genoemde ellipsoïden, berekend worden. Deze versnellingen blijken kleiner te zijn dan de versnellingen, die afgeleid kunnen worden uit de in het stelsel waargenomen rotatiesnelheden. Om nu de versnellingen in het model in overeenstemming met de waarnemingen te brengen, is er een vierde ellipsoïde aan het model toegevoegd. Het dichtheidsverloop in deze ellipsoïde, die dus onbekende objecten bevat, kan berekend worden. Het blijkt dat deze objecten ongeveer de helft van de massa van het Melkwegstelsel leveren, sterk geconcentreerd zijn naar het symmetrievlak van het stelsel en bij de zon een hoge relatieve dichtheidsgradient vertonen.